Int. J. Solids Structures Vol. 27, No. 1, pp. 105–133, 1991
Printed in Great Britain.

0020-7683/91 $3.00 + .00

STABLE CRACK GROWTH ALONG A BRITTLE/DUCTILE INTERFACE—I. NEAR-TIP FIELDS

P. PONTE CASTAÑEDA
Department of Mechanical Engineering, The Johns Hopkins University, Baltimore, MD 21218, U.S.A.

and

P. A. MATAGA†
Materials Department, University of California, Santa Barbara, CA 93106, U.S.A.

(*Received* 25 *July* 1989; *in revised form* 11 *December* 1989)

Abstract—In Part I of this work the asymptotic near-tip stress and velocity fields of a crack propagating steadily and quasi-statically along the interface between a ductile and a brittle material are presented. The ductile material is characterized by J_2-flow theory with either linear hardening or ideal plasticity. The brittle material is characterized by linear elastic behavior. The cases of anti-plane strain and plane strain are considered.

The linear-hardening solutions are assumed to be of variable-separable form with a power singularity in the radial distance to the crack tip. Results are given for the strength of the singularity and for the distribution of the stress and velocity fields as functions of the hardening parameter. However, the amplitude of the fields, or plastic stress intensity factor, is left undetermined by this asymptotic analysis. For the case of plane strain, it is found that two distinct solutions exist with slightly different singularity strengths, and very different mixities on the interfacial line ahead of the crack. For hardening small enough, one of the solutions corresponds to a tensile-like mode, whereas the other solution corresponds to a shear-like mode. These two solutions coalesce at an intermediate value of the hardening, if a certain bimaterial parameter is not zero. In this case, no variable-separable solutions are found for larger values of the hardening parameter. On the other hand, if the bimaterial constant vanishes, the two solutions remain distinct for all values of the hardening parameter up to the perfectly-elastic limit.

The ideally plastic solutions are obtained by means of an appropriate assembly of elastic unloading and active plastic sectors, the latter being of either centered-fan or constant-stress type. For simplicity, the substrate material is assumed to be rigid, and the ductile material to be incompressible. The perfectly-plastic results for the stress and velocity fields in this case are continuous and consistent with the small-hardening results showing a tensile- as well as a shear-like solution.

In Part II of this work, the corresponding small scale yielding problem will be solved numerically, and the relevance of the asymptotic solutions will be investigated. Where appropriate, the plastic stress intensity factors corresponding to the asymptotic solutions will be determined as functions of the elastic stress intensity factor and the mixity of the applied fields. This information will be useful in determining "resistance curves" for crack growth along brittle/ductile interfaces.

1. INTRODUCTION

Interfaces between brittle and ductile materials are present in many important composite materials, from cermets and other modern structural ceramics to packaging structures for electronic devices. It is often the case that such materials fail by the *propagation* and coalescence of pre-existing or "nucleated" cracks along these interfaces. Thus, the propagation of microscopic and macroscopic cracks along interfaces between brittle and ductile materials can be an important factor in determining the overall strength, toughness and reliability of composite materials with brittle and ductile phases. It is also possible, however, that a given crack at the interface would find it energetically favorable to branch off the interface and penetrate into either the brittle or the ductile phase, but if the interface is

† Currently at the Department of Aerospace Engineering, Mechanics and Engineering Science, University of Florida, Gainesville, FL 32611, U.S.A.

assumed to be inherently weaker than both materials, then the crack would most likely propagate *along* the interface. This assumption is implicitly made in this work.

The main objective of this work is to study the steady and quasi-static propagation of anti-plane and plane strain cracks along interfaces between brittle and ductile materials under small scale yielding conditions. The work is divided into two parts: the first part, which is the subject of this paper, deals with the determination of the asymptotic stress and deformation fields near the tip of the growing crack, and the second, which is to be addressed in the sequel, makes use of the finite element method to produce the corresponding full-field, small scale yielding solutions.

The results of this work would be useful in the theoretical prediction of "resistance curves" for stable crack growth along brittle/ductile interfaces. This phenomenon, which is well documented (Green and Knott, 1975) for the propagation of cracks in homogeneous ductile materials under slowly increasing external loading, is of great practical significance, because for these materials the level of external loading required to propagate a given crack unstably, and hence ultimately break the structure, can be many times the level required for the initiation of crack growth. Therefore, a detailed understanding of this phenomenon is desirable to make a more efficient use of materials in the design of structural components which are prone to failure by crack growth. Essential to the understanding of this phenomenon is the determination of the asymptotic near-tip fields associated with a propagating crack. This knowledge can not only give direct partial information about the structure of the phenomenon, but can also be used in conjunction with numerical analyses of practical configurations to gain a more detailed understanding of the process as a whole. It will be assumed in this work that the same phenomenon applies to crack growth along brittle/ductile interfaces through essentially the same mechanism of plastic dissipation in the ductile half of the composite material. The authors are not aware of any published experimental work in this area.

Due to the analytical difficulties involved, the bulk of the research on near-tip asymptotic fields has been associated with homogeneous materials, characterized by infinitesimal flow theory with either linear-hardening or perfect plasticity. Rice (1982) presented a complete analysis of the asymptotic structure of the near-tip stress and deformation fields of a crack growing quasi-statically into an elastic/perfectly-plastic solid, including explicit solutions of the governing equations for anti-plane strain, plane strain and plane stress. This reduces the perfectly-plastic problem to that of finding an appropriate assembly of elastic and plastic sectors satisfying certain continuity and boundary conditions. In anti-plane strain, the first successful assembly of sectors for a Mises material was given by Chitaley and McClintock (1971). In plane strain, Slepyan (1974) presented the corresponding assembly of sectors for the Tresca material in both modes I and II. Independently, Gao (1980) and Rice *et al.* (1980) produced results for the Mises material in mode I ($\nu = 1/2$), and Drugan *et al.* (1982) generalized these results to the case of $\nu \neq 1/2$. Ponte Castañeda (1986) gave a solution for the mode II plane stress problem. The corresponding linear-hardening problems were addressed by Slepyan (1973), who considered anti-plane strain crack growth in a modified deformation-theory material; by Amazigo and Hutchinson (1977), who considered anti-plane strain, as well as plane stress and plane strain, crack growth in a J_2-flow theory material, but neglected plastic reloading; and by Ponte Castañeda (1987a), who extended the work of the previous authors to include reloading and mode II solutions. All of these asymptotic solutions leave certain parameters undetermined in the expressions for the stress and deformation fields near the tip of the moving crack. In the perfectly-plastic case, the parameter in question is the size of the plastic zone ahead of the crack, but this parameter does not appear in the lowest-order term of the asymptotic expansion of the fields, and its determination is not essential. On the other hand, in the linear-hardening case the amplitude of the lowest-order term of the asymptotic expansion for the stress and deformation fields, or *plastic* stress intensity factor, is undetermined from the asymptotic analysis, and its determination is an important problem. Under the assumption of small scale yielding, this problem was addressed by means of an approximate variational technique by Ponte Castañeda (1987b). Other related full-field studies addressing different types of constitutive behavior include the finite element

works of Dean and Hutchinson (1980), Parks *et al.* (1981), Sham (1983) and Narasimham *et al.* (1987).

The understanding of interfacial fracture is at a much earlier stage of development, and thus the bulk of the work has dealt with stationary cracks in linear-elastic materials, building on the basic contributions of Williams (1959), England (1965), Erdogan (1965), Rice and Sih (1965), Willis (1971) and Comninou (1977). For a review of some of the more recent contributions, the reader is referred to the papers by Rice (1988) and Hutchinson (1989). The first contributions dealing with material nonlinearities include the plane stress work of Knowles and Sternberg (1983), addressing finite deformations, and the work of Shih and Asaro (1988, 1989), and Parks and Zywicz (1989) (see also Zywicz, 1988), dealing with power-law hardening, and perfectly-plastic behavior, respectively. In the context of crack propagation, very few contributions can be counted at this time: the early work by Willis (1971), who applied the local form of the Griffith virtual work criterion to cracks propagating along the interface between dissimilar anisotropic elastic materials; and more recent work by Hutchinson *et al.* (1987), who considered the possibility of crack propagation paralleling an interface between dissimilar elastic materials. To the knowledge of the authors, no contributions concerning crack propagation along interfaces between nonlinear materials have yet appeared in the literature†, and in this regard this work constitutes one of the first contributions in this area.

This part of the work is divided into two main sections dealing with the determination of the asymptotic near-tip stress and velocity fields associated with crack propagation along the interface between a brittle and a linear-hardening material, or between a brittle and a perfectly-plastic material, under anti-plane and plane strain conditions, respectively. The procedure used in the solution of the linear-hardening problem follows the formulation developed by Ponte Castañeda (1987a), and the procedure used in the perfectly-plastic problem follows the work of Rice (1982).

2. ANTI-PLANE STRAIN

2.1. *Formulation of the linear-hardening problem*

Figure 1a refers to a two-dimensional crack propagating steadily and quasi-statically along the interface between a ductile material on the upper half (denoted material No. 1), and a brittle material on the lower half (denoted material No. 2). Let x_i ($i = 1, 2, 3$) be a Cartesian coordinate system of fixed orientation travelling with the crack front in such a way that the x_3 axis coincides with the straight crack front at all times. Also let $\mathbf{e}_i$ be the unit vector corresponding to the x_i direction. Similarly, let r, θ be polar coordinates corresponding to x_α ($\alpha = 1, 2$) and $\mathbf{e}_r$, $\mathbf{e}_\theta$ be the corresponding unit vectors. The crack tip moves with velocity $\mathbf{V} = V\mathbf{e}_1$ with respect to the stationary coordinate system X_i. In our steady-state analysis, the crack-tip speed V is constant, and therefore the material derivative of any field quantity is given by

$$\dot{(\,)} = -V(\,)_{,1} \tag{1}$$

It should be noted that this relation still holds in an asymptotic sense when the motion of the crack front is non-uniform, but quasi-static.

The dependent variables of this problem are the anti-plane shear stresses $\tau_\alpha = \sigma_{\alpha 3}$ and the anti-plane velocity v_3, which are functions of the in-plane coordinates x_α only. In terms of the polar components of the stress vector τ and the velocity v_3, the equation of equilibrium

†The present work, as well as related work by W. J. Drugan on ideally plastic solutions for growing interfacial cracks, and by P. G. Charalambides *et al.* on the mechanics of a growing crack paralleling an elastically constrained thin ductile layer, were reported at the Third Joint ASCE/ASME Mechanics Conference, held at the University of California, San Diego, 9–12 July 1989.

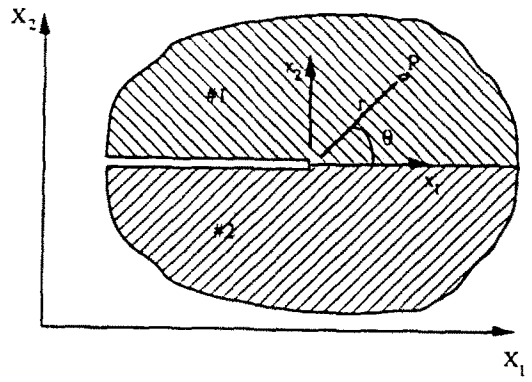

Fig. 1a. Crack-tip geometry.

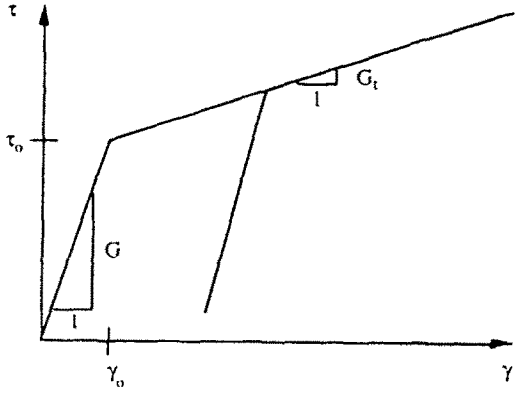

Fig. 1b. Stress–strain curve in shear for the ductile material.

takes the form

$$(r\tau_r)_{,r} + \tau_{\theta,\theta} = 0, \tag{2}$$

where we have used the fact that the inertial and body forces in this problem are zero.

In this section, we assume that the constitutive response of the ductile material on the upper half of the interface is characterized by J_2-flow theory of plasticity with a bilinear stress–strain curve in shear as shown in Fig. 1b. Thus, the stress–strain relation for this material under general loading is given by

$$\mathbf{G} = (1/G^{(1)})\,[\mathbf{T} + \dot{\Lambda}\boldsymbol{\tau}], \tag{3}$$

where

$$\dot{\Lambda} = (\alpha^{-1} - 1)(\dot{\tau}_e/\tau_e).$$

$\mathbf{G} = \nabla v_1$ is the engineering strain-rate vector, $\mathbf{T} = \dot{\boldsymbol{\tau}}$ is the stress-rate vector, $\tau_e = |\boldsymbol{\tau}|$ is the effective stress, and α is either α or unity, depending on whether the given material point is in an *active* plastic zone or in a region of elastic behavior, respectively. Here $\alpha = G_t^{(1)}/G^{(1)}$, the ratio of the tangent modulus to the elastic modulus in shear of material No. 1, is the appropriate hardening parameter.

As noted by Ponte Castañeda (1987a), (2) and (3) form a system of three first-order PDEs in the two stress components and the single velocity component that are homogeneous in the radial measure r and therefore it is sensible to look for variable-separable asymptotic solutions of the form

$$\tau_r(r,\theta) = K_{pl}\, y_1(\theta)\,(2\pi r)^s, \quad \tau_\theta(r,\theta) = K_{pl} y_2(\theta)(2\pi r)^s, \quad v_3(r,\theta) = K_{pl}(V/G^{(1)})\, y_3(\theta)(2\pi r)^s/s, \tag{4}$$

where the peculiar choice for the radial dependence of the velocity (r^s/s) is made so that the corresponding angular variations remain bounded as $\alpha \to 0$, and where the plastic stress intensity factor K_{pl}, defined by

$$K_{pl} = \lim_{r\to 0} (2\pi r)^{-s}\tau_\theta(r,0),$$

is undetermined by the asymptotic analysis. Ponte Castañeda (1987b) has shown that the plastic stress intensity factor of a steadily propagating crack in a homogeneous material of the type described above under small scale yielding conditions is given by

$$K_{pl} = \kappa(\alpha)(\tau_0)^{1+2s}(K_{el})^{-2s},$$

where τ_0 is the yield stress in shear, K_{el} is the applied elastic stress intensity factor, and κ is a dimensionless parameter depending on α that needs to be determined from the solution of the full small scale yielding problem. We expect analogous results for the present problem, and this will be addressed in Part II of this work.

Putting expressions (4) into (2) and (3) results in a system of three first-order ODEs in the vector $\mathbf{y} = (y_1, y_2, y_3)$ such that

$$\mathbf{y}'(\theta) = \mathbf{f}(\theta, \mathbf{y}; s, \underline{\alpha}), \quad (0 < \theta \leqslant \pi), \tag{5}$$

where the components of the vector function $\mathbf{f}$ are given in Appendix A. The parameter α is in turn determined by the functions

$$\begin{aligned} y_e(\theta) &= [y_1^2(\theta) + y_2^2(\theta)]^{1/2}, \\ \phi(\theta) &= r\dot{\tau}_e/\tau_e = -s\cos\theta + \sin\theta[y_e'(\theta)/y_e(\theta)], \end{aligned} \tag{6}$$

in such a way that unloading ($\underline{\alpha}$ jumps from α to 1) occurs at θ_1, when the effective stress-rate of the particle vanishes, or when

$$\phi(\theta_1) = 0, \tag{7}$$

and reloading ($\underline{\alpha}$ jumps from 1 to α) occurs at θ_2, if the effective stress of the particle regains its unloading value, or if

$$y_e(\theta_1)/(\sin\theta_1)^s - y_e(\theta_2)/(\sin\theta_2)^s = 0. \tag{8}$$

The solutions in the different regions need to be connected through appropriate continuity conditions across the boundaries between such regions. It can be shown (Ponte Castañeda, 1987a) that the stresses and the anti-plane velocity must be continuous across the unloading and reloading boundaries. Denoting by [ ] the jump in a field as θ increases infinitesimally across such a boundary, this implies that the angular variations of the fields must satisfy

$$[y_1] = [y_2] = [y_3] = 0. \tag{9}$$

In the lower half of the interface, the governing equations are the equilibrium equation (2), and the linear stress–strain relation corresponding to an elastic material. This stress–strain relation can be considered a special case of (3) with $\alpha = 1$, and no residual plastic strains. For this reason, and also for asymptotic consistency, the resulting fields in the lower half will also have the variable-separable form (4) with the same singularity s, but here the

velocity needs to be normalized with respect to the elastic modulus in shear of the brittle material, $G^{(2)}$. The corresponding ODEs associated with these equations can then be solved explicitly for the angular variations of the fields. The result is

$$\begin{aligned} y_1(\theta) &= -(B/s)\cos[s(\theta-\delta)-\theta], \\ y_2(\theta) &= (B/s)\sin[s(\theta-\delta)-\theta], \quad (-\pi \leqslant \theta < 0), \\ y_3(\theta) &= B\cos s(\theta-\delta), \end{aligned} \tag{10}$$

where B and δ are arbitrary constants.

The statement of the problem is completed by the specification of the boundary conditions on the crack faces ($\theta = \pm\pi$), and the appropriate jump conditions across the brittle ductile interface ($\theta = 0$). The first set of conditions which requires that the traction stress vanishes on the crack faces, reduces to

$$y_2(\pm\pi) = 0. \tag{11}$$

The second set which requires the continuity of the traction stress and of the displacement, reduces to

$$\begin{aligned} y_2(0+) &= y_2(0-), \\ y_3(0+) &= \beta y_3(0-), \end{aligned} \tag{12}$$

where $\beta = G^{(1)}/G^{(2)}$, and where in the derivation of the second equality, we have made use of the fact that, on the line ahead of the crack, displacement continuity implies velocity continuity. Note that the first equality was implicit in the definition of the plastic stress intensity factor K_{pl}. Also implicit in this definition is the normalization,

$$y_2(0) = 1, \tag{13}$$

for the angular variations of the stress and deformation fields.

The second of conditions (11), and condition (13) suffice to completely specify the fields in the brittle material ($-\pi \leqslant \theta < 0$) by determining $B = s/\sin(s\pi)$ and $\delta = -\pi$. This result can then in turn be used in combination with conditions (12) to specify the boundary values of the fields on the upper half at $\theta = 0+$. The final result is

$$\begin{aligned} y_1(0+) &= -\alpha\beta\cot(s\pi), \\ y_2(0+) &= 1, \\ y_3(0+) &= s\beta\cot(s\pi), \end{aligned} \tag{14}$$

where we have also made use of the stress–strain relation for the ductile material in establishing the first condition above.

This new problem of a crack propagating along a brittle/ductile interface is formally similar to the problem solved by Ponte Castañeda (1987a) for the crack propagating in a homogeneous linear-hardening material; the only difference being that the boundary conditions on the crack line are not those of mode III symmetry, but instead the more complicated conditions specified by (14). Thus the new problem reduces to solving the nonlinear eigenvalue problem specified by the third-order system (5) subject to the boundary conditions (14) on the interfacial line and the boundary condition (11) on the upper face of the crack. This problem is to be solved for the eigenvalue s and the system of eigenfunctions $\mathbf{y}(\theta)$ for given values of the parameters α and β. Because the boundary conditions (14) are not homogeneous, it is not obvious that this is a well-posed eigenvalue problem. However, it can be easily verified that if $\mathbf{y}$ is a solution corresponding to the normalization $y_2(0) = 1$, then $\tilde{\mathbf{y}} = A\mathbf{y}$ is also a solution corresponding to the normalization $y_2(0) = A$.

This follows from the homogeneity of the system (5) in $\mathbf{y}$, and the nature of the boundary and interfacial conditions. The boundary condition on the crack face is clearly homogeneous, and the conditions on the interfacial line are such that the angular variations of the fields $\mathbf{y}(\theta)$ are linearly related to each other. Furthermore, it is not difficult to verify that the problem on the lower half is a regular Sturm–Liouville problem for y_3 with $y_3''+s^2y_3=0$, subject to a homogeneous boundary condition $y_3'(-\pi)=0$ at the lower crack face, and a boundary condition of the form $y_3'(0+)+\eta y_3(0+)=0$ on the interfacial line, where η is determined by the solution of the problem on the upper half.

The above eigenvalue problem is solved by means of a shooting method making use of a Runge–Kutta–Verner fifth- and sixth-order scheme to perform the relevant numerical integrations. Thus we guess the value of s for given α and β, and hence determine the initial values of the dependent variables $\mathbf{y}(0+)$ through (14). We then integrate eqns (5) to find the values of $\mathbf{y}(\theta)$ for $0<\theta\leqslant\pi$, checking to determine when unloading and reloading occur in order to make use of the appropriate value of α. Once we have the values of $\mathbf{y}(\pi)$, we check to see whether $y_2(\pi)$ is zero, and we iterate in our guess for s until convergence is achieved by means of an appropriate numerical scheme.

Note, however, that we cannot use (5) to find directly the values of $y_1'(0+)$, but we can easily take the appropriate limits analytically to find that

$$\begin{aligned} y_1'(0+) &= \frac{1+s+\lambda(1-s^2/\alpha)}{1+\lambda(1-s/\alpha)}, \\ y_2'(0+) &= \alpha/\beta(1+s)\cot(s\pi), \\ y_3'(0+) &= -s^2/\alpha, \end{aligned} \tag{15}$$

where

$$\lambda=\left(\frac{\alpha}{1-\alpha}\right)\left(1+\frac{\tan^2(s\pi)}{(\alpha\beta)^2}\right).$$

Similarly, note that eqns (5) are numerically ill-conditioned at $\theta=\pi$, but we can integrate them to $\theta=\pi-\varepsilon$, and make ε as small as necessary. Since $y_2(\theta)$ is well-behaved near $\theta=\pi$, this approximation yields results as accurate as needed. Finally, we note that, for the purpose of comparison with the results of Ponte Castañeda (1987a), the final results depicted in the following subsection are renormalized such that

$$y_e(\theta_1)=1. \tag{16}$$

2.2. *Linear-hardening results*

The results of this section are summarized in Tables 1 and Figs 2 and 3. Figure 2 is a plot of the strength of the singularity, s, versus the square root of the hardening parameter,

Table 1a. Strength of the singularity, unloading and reloading angles versus hardening in anti-plane strain ($\beta=1$)

α	s	θ_1	θ_2
0.8	−0.48173	88.600	
0.6666	−0.46594	87.703	
0.5	−0.43928	86.486	
0.3	−0.38725	84.280	
0.2	−0.34339	82.144	
0.1	−0.26952	77.609	
0.05	−0.20419	72.406	
0.01	−0.09937	60.761	179.999
0.005	−0.07166	56.609	179.970
0.001	−0.03297	49.301	179.910
0.0001	−0.01064	43.274	179.843

Table 1b. Strength of the singularity, unloading and reloading angles versus hardening in anti-plane strain ($\beta=0$)

α	s	θ_1	θ_2
0.8	−0.46487	88.300	
0.6666	−0.43689	86.829	
0.5	−0.39444	84.386	
0.3	−0.32529	79.808	
0.2	−0.27676	76.085	
0.1	−0.20711	69.824	
0.05	−0.15297	63.980	179.999
0.01	−0.07325	52.874	179.947
0.005	−0.05285	49.206	179.912
0.001	−0.05285	42.884	179.840
0.0001	−0.00792	37.674	179.776

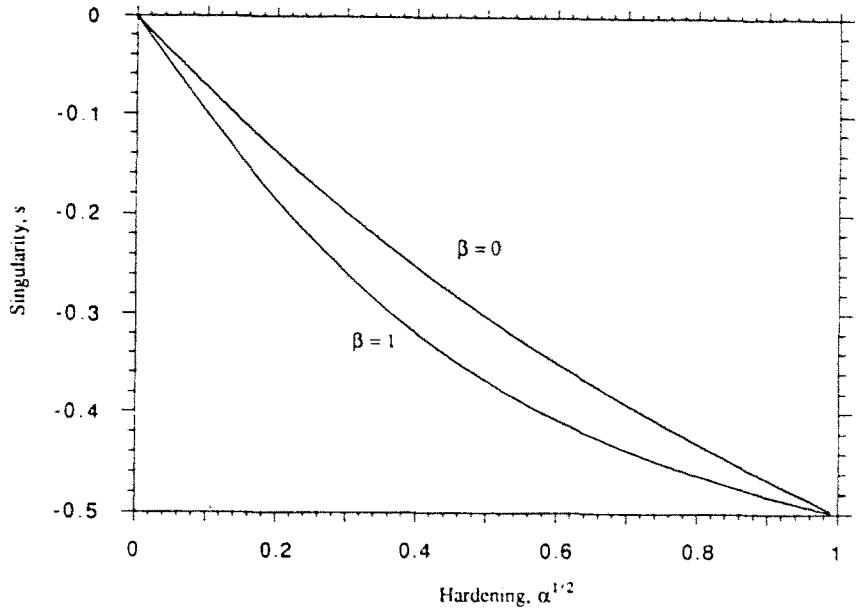

Fig. 2. Strength of the singularity as a function of hardening in anti-plane strain for two values of β.

α, for two values of the ductile to brittle ratio of elastic moduli ($\beta = 0$ and 1). It can be seen that s is significantly stronger for $\beta = 1$ that for $\beta = 0$. It is worth mentioning that the case of $\beta = 0$ corresponds exactly to the case of the propagating crack in a homogeneous linear-hardening medium. This is due to the well-known symmetries of the mode III problem. Also, as for the homogeneous linear-hardening material, it is observed that $s \sim -\alpha^{1/2}$ for small α.

Tables 1 present values of s, θ_1 and θ_2 for $10^{-4} \leqslant \alpha < 1$, and the two values of β mentioned above. It is found that reloading occurs for $0 < \alpha < \alpha^*$ for values of α^* ranging between 0.01 and 0.05, depending on the specific value of β. For $\alpha^* < \alpha < 1$ a two-region (loading/unloading) solution exists, and for $0 < \alpha < \alpha^*$ this solution switches over to a three-region (loading/unloading/reloading) solution, where the reloading sector is very small.

Figures 3 present plots of the angular (fixed r) variations of the stresses and velocity for the two above values of β, and for a small value of the hardening ($\alpha = 0.001$). We note that the difference in the distribution of the fields for a larger value of the hardening is not very significant, but for small enough hardening the characteristic distribution of the perfectly-plastic solution of Chitaley and McClintock (1971) is clearly observed. Also, interestingly, changing the value of β only seems to affect significantly the velocity distribution in the centered-fan sector, and not elsewhere.

2.3. *Perfectly-plastic results*

The problem of a crack propagating along the interface between a perfectly-plastic material and elastic material is an important problem that merits a thorough investigation. In the present study, however, we will be satisfied with presenting results for a particularly simple special case for the purpose of comparison with our linear-hardening results. The special case in point is that of a crack propagating along the interface between an elastic/perfectly-plastic solid and a rigid substrate corresponding to a zero value of β. This case is of practical interest, and its solution can be obtained by reinterpreting the solution of Chitaley and McClintock (1971) for the homogeneous elastic/perfectly-plastic solid. Obviously, this solution satisfies the boundary condition on the upper face of the crack, and, additionally, satisfies the appropriate interfacial conditions in the line ahead of the

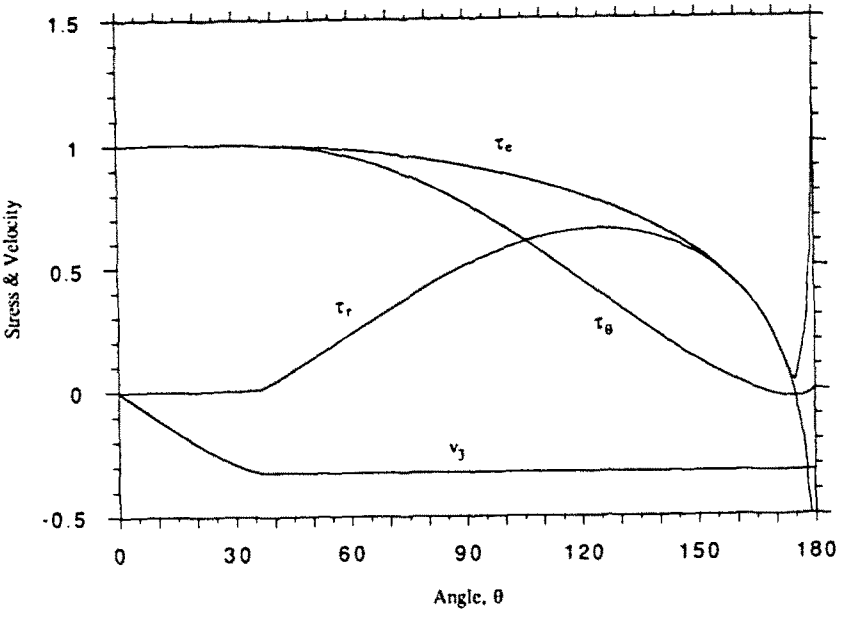

Fig. 3a. Angular variations of the stress and velocity fields in anti-plane strain for small hardening ($\alpha = 0.001$) and $\beta = 0$.

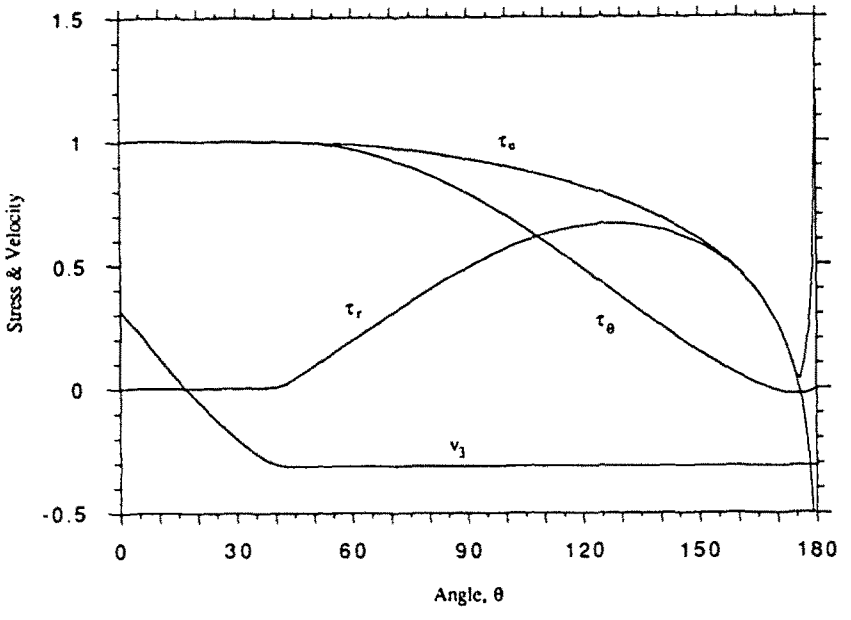

Fig. 3b. Angular variations of the stress and velocity fields in anti-plane strain for small hardening ($\alpha = 0.001$) and $\beta = 1$.

crack. Thus, the anti-plane velocity vanishes in the interfacial line, as it should by continuity with respect to a rigid substrate. On the other hand, we do not need to worry about the stress conditions because the rigid substrate will accommodate trivially any level of shear stress arising from the condition of traction continuity. Hence, the solution of the interfacial perfectly-plastic growing crack with $\beta = 0$ is given by the Chitaley and McClintock fields on the upper half, and a trivial velocity distribution on the lower rigid half. These results are given in Appendix B. Also, as mentioned in the previous section, the corresponding linear-hardening results for $\beta = 0$ are identical to the homogeneous linear-hardening results

of Ponte Castañeda (1987a), and therefore we refer the reader to that work to infer the appropriate comparisons between the linear-hardening and perfectly-plastic interfacial growing-crack solutions. We will simply remark here that under the normalization of the radial dependence of the velocity prescribed in the previous section (r^s's), not only do the angular variations of the stresses in the linear-hardening problem appear to approach those of the perfectly-plastic problem, but the same behavior is also observed for the corresponding angular variations of the velocity.

3. PLANE STRAIN

3.1. *Formulation of the linear-hardening problem*

The same configuration of Fig. 1a with the obvious generalizations applies to this problem, and hence eqn (1) also holds here. On the other hand, the dependent variables of this problem are the in-plane stress components $\sigma_{\alpha\beta}$, the out-of-plane normal stress component σ_{33}, and the in-plane velocity components v_α. Alternatively, we can also make use of the corresponding cylindrical components of the stress tensor $\boldsymbol{\sigma}$ and of the velocity vector $\mathbf{v}$. Noting that under the plane strain assumption, these variables are functions only of the in-plane coordinates x_α, the quasi-static equilibrium equations reduce to

$$(r\sigma_{rr})_{,r} + \sigma_{r\theta,\theta} - \sigma_{\theta\theta} = 0, \tag{17}$$

$$(r\sigma_{r\theta})_{,r} + \sigma_{\theta\theta,\theta} + \sigma_{r\theta} = 0. \tag{18}$$

For a bilinear flow theory solid in the upper half, the appropriate stress–strain relation is

$$\mathbf{D} = (1/E^{(1)})[(1+\nu^{(1)})\boldsymbol{\Sigma} - \nu^{(1)}\, Tr\,(\boldsymbol{\Sigma})\mathbf{I} + \dot{\Lambda}\mathbf{S}], \tag{19}$$

where

$$\dot{\Lambda} = (3/2)(\alpha^{-1} - 1)(\dot{\sigma}_e/\sigma_e),$$

$\mathbf{D} = (1/2)[\nabla\mathbf{v} + (\nabla\mathbf{v})^t]$ is the rate-of-deformation tensor, $\boldsymbol{\Sigma} = \dot{\boldsymbol{\sigma}}$ is the stress-rate tensor, $\mathbf{S} = \boldsymbol{\sigma} - (1/3)\, Tr\,(\boldsymbol{\sigma})\mathbf{I}$ is the stress-deviator tensor, $\sigma_e = [(3/2)\mathbf{S}:\mathbf{S}]^{1/2}$ is the effective stress, $\mathbf{I} = \mathbf{e}_i\mathbf{e}_i$ is the identity tensor, $\nu^{(1)}$ is Poisson's ratio for the ductile material No. 1 and α is either α or unity depending on whether plastic loading, elastic unloading or reloading takes place. Here $\alpha = E_t^{(1)}/E^{(1)}$, the ratio of the tangent modulus in tension to Young's modulus for the ductile material, is the appropriate hardening parameter.

Note that eqns (19) contain only four non-trivial equations (including the plane strain condition $D_{33} = 0$). Therefore, eqns (17), (18) and (19) form a system of six first-order PDEs in the six dependent variables identified above. As in anti-plane strain, all six equations are homogeneous in r, which again suggests that we look for asymptotic solutions of variable-separable form

$$\begin{aligned}
v_r(r,\theta) &= K_{pl}(V/E^{(1)})y_1(\theta)(2\pi r)^s/s, \quad v_\theta(r,\theta) = K_{pl}(V/E^{(1)})y_2(\theta)(2\pi r)^s/s,\\
\sigma_{r\theta}(r,\theta) &= K_{pl}y_3(\theta)(2\pi r)^s, \qquad \sigma_{rr}(r,\theta) = K_{pl}y_4(\theta)(2\pi r)^s,\\
\sigma_{\theta\theta}(r,\theta) &= K_{pl}y_5(\theta)(2\pi r)^s, \qquad \sigma_{33}(r,\theta) = K_{pl}y_6(\theta)(2\pi r)^s,
\end{aligned} \tag{20}$$

where the plastic stress intensity factor K_{pl} is now defined by

$$K_{pl} = \lim_{r\to 0}(2\pi r)^{-s}\sigma_{\theta\theta}(r,0),$$

and is again undetermined by the asymptotic analysis. Under small scale yielding conditions, we expect this plastic stress intensity factor to depend on the yield stress and the applied elastic stress intensity factors in a way to be elucidated in Part II of this work.

Putting the proposed solutions (20) into eqns (17)–(19), we obtain a system of six first-order ODEs in the vector $\mathbf{y} = (y_1, y_2, \ldots, y_6)$

$$\mathbf{y}'(\theta) = \mathbf{f}(\theta, \mathbf{y}; s, v^{(1)}, \underline{\alpha}), \quad (0 < \theta \leqslant \pi), \tag{21}$$

where the components of $\mathbf{f}$ are given in Appendix A, and depend on the parameter $\underline{\alpha}$, whose value is in turn determined by the unloading condition

$$\dot{\phi}(\theta_1) = 0, \tag{22}$$

and the reloading condition

$$y_\epsilon(\theta_1)/(\sin\theta_1)^s - y_\epsilon(\theta_2)/(\sin\theta_2)^s = 0, \tag{23}$$

where $y_\epsilon(\theta)$ and $\dot{\phi}(\theta)$ have been appropriately redefined.

These conditions are supplemented by appropriate stress and velocity continuity conditions across the unloading and reloading boundaries. In the notation of the previous section, they take the form

$$[y_1] = [y_2] = \ldots = [y_6] = 0. \tag{24}$$

In the lower half of the interface, the governing equations are the equilibrium equations (17) and (18), and the linear stress–strain relations corresponding to an elastic material. For the same reasons as for anti-plane strain, we assume solutions of the form (20) in the lower half, with the only difference that in this case the velocities are normalized with respect to the Young's modulus for the brittle material, E^2. The exact solution of these equations can be obtained by complex-variable methods in terms of Muskhelishvili potentials proportional to ω^s (where $\omega = x_1 + \mathrm{i}x_2$ is a complex variable), as in Ponte Castañeda (1987c). This leads to the following result for the angular variations of the Cartesian components of the fields z_i $(i = 1, \ldots, 6)$ (corresponding to v_1, v_2, σ_{12}, σ_{11}, σ_{22}, σ_{33}, respectively):

$$\begin{aligned}
z_1(\theta) &= -s(1+v^{(2)})A\{(\kappa^{(2)}+s)\cos(s\theta-\gamma) - s\cos[(s-2)\theta-\gamma] + \cos[s(\theta+2\pi)+\gamma]\},\\
z_2(\theta) &= -s(1+v^{(2)})A\{(\kappa^{(2)}-s)\sin(s\theta-\gamma) + s\sin[(s-2)\theta-\gamma] - \sin[s(\theta+2\pi)+\gamma]\},\\
z_3(\theta) &= A\{s\sin[(s-2)\theta-\gamma] - (s+1)\sin(s\theta-\gamma) - \sin[s(\theta+2\pi)+\gamma]\},\\
z_4(\theta) &= A\{-s\cos[(s-2)\theta-\gamma] + (s+3)\cos(s\theta-\gamma) + \cos[s(\theta+2\pi)+\gamma]\},\\
z_5(\theta) &= A\{s\cos[(s-2)\theta-\gamma] - (s-1)\cos(s\theta-\gamma) - \cos[s(\theta+2\pi)+\gamma]\},\\
z_6(\theta) &= v^{(2)}\{z_4(\theta) + z_5(\theta)\},
\end{aligned} \tag{25}$$

valid for $-\pi \leqslant \theta < 0$, where A and γ are arbitrary constants, $\kappa^{(2)} = 3 - 4v^{(2)}$ for plane strain, and where we have already imposed the traction-free conditions on the lower face of the crack

$$y_3(-\pi) = y_5(-\pi) = 0.$$

It remains to impose the traction-free conditions on the upper face of the crack

$$y_3(\pi) = y_5(\pi) = 0, \tag{26}$$

and also to enforce continuity of the tractions and velocities across the interfacial line ahead of the crack, which requires that

$$y_1(0+) = \beta y_1(0-),$$
$$y_2(0+) = \beta y_2(0-),$$
$$y_3(0+) = y_3(0-),$$
$$y_5(0+) = y_5(0-), \tag{27}$$

where $\beta = E^{(1)}/E(2)$ is the ratio of the Young's moduli of the two materials. Note that the fourth equality was implicit in the definition of the plastic stress intensity factor, as is the normalization

$$y_5(0) = 1.$$

These conditions, together with the solutions in the lower half (25), allow the determination of the values of $y_1(0+)$, $y_2(0+)$, $y_3(0+)$ and $y_5(0+)$ in terms of s, α, β, γ, $\nu^{(1)}$ and $\nu^{(2)}$. Likewise, the stress–strain relations for the ductile material on the upper half allow the determination of $y_4(0+)$ and $y_6(0+)$ in terms of the expressions

$$y_4(0+) = -\alpha\{y_1(0+)/s - \lambda[y_5(0+) + y_6(0+)]\},$$
$$y_6(0+) = \alpha\lambda[y_4(0+) + y_5(0+)], \tag{28}$$

with $\lambda = \nu^{(1)} + (\alpha^{-1} - 1)/2$, which are obtained by considering the limit as $\theta \to 0+$ of the expressions for D_{rr} and D_{33} in (19) with r fixed. It should be noted that the dependence of $\mathbf{y}(0+)$ on γ is π-periodic, and therefore only values of $\gamma \in [-\pi/2, \pi/2]$ need to be considered.

Thus we have reduced this interfacial crack problem to a problem with exactly the same form as the corresponding problem for the propagating crack in a homogeneous linear-hardening material considered by Ponte Castañeda (1987a), with the difference that the conditions in the line ahead of the crack are not those of mode I symmetry or mode II antisymmetry, but instead these conditions take the more complicated, yet explicit form, discussed above. By arguments similar to those made in the anti-plane strain section, we are left with a nonlinear eigenvalue problem specified by the sixth-order system (21) subject to the six conditions (27) and (28) on the interfacial line ahead of the crack, and the two conditions (26) on the upper face of the crack. This eigenvalue problem is to be solved for the strength of the singularity s, the "mixity" angle γ, and the angular variations of the fields $\mathbf{y}(\theta)$ for given values of the hardening parameter α, the ratio of the Young's moduli β and the Poisson's ratios $\nu^{(1)}$ and $\nu^{(2)}$. It is important to note the appearance of this new mixity parameter which is to be determined by the above procedure. This feature has the physical significance that, if the only solutions of the problem are of the assumed form (20), then the mixity of the fields in the near-tip limit is determinate, and cannot be prescribed arbitrarily as is the case for the corresponding stationary crack problem. This is not a feature intrinsic to the *interfacial* crack; in fact, Ponte Castañeda and Bose (1990) have made analogous observations for the growing crack in the *homogeneous* linear-hardening material (in this problem the only admissible solutions appear to be the symmetric mode I and the antisymmetric mode II solutions). The practical significance of this feature will need to be assessed from the numerical solutions of the full small scale yielding problem by analyzing the behavior of the near-tip fields under the prescription of arbitrary mixities of the remote applied elastic fields. This will be carried out in Part II of this study.

Because the mixity angle γ is hard to visualize, we introduce, following Shih (1974), a plastic mixity parameter related to γ

$$m_{\mathrm{pl}} = \frac{2}{\pi}\tan^{-1}\left(\lim_{r\to 0}\frac{\sigma_{\theta\theta}(r,0)}{\sigma_{r\theta}(r,0)}\right). \tag{29}$$

This parameter, which has a period of 2, is such that $m_{\mathrm{pl}} = 1$ for pure mode I and $m_{\mathrm{pl}} = 0$ for pure mode II.

Concerning the well-posedness of this eigenvalue problem, it is important to note that in the elastic limit ($\alpha = 1$), the corresponding stress singularity (Williams, 1959) is complex of the form $s = -1/2 + i\varepsilon$, so that variable-separable solutions of the form (20) exist only if the bimaterial constant

$$\varepsilon = (1/2\pi) \ln [(\kappa^{(1)}/G^{(1)} + 1/G^{(2)})/(\kappa^{(2)}/G^{(2)} + 1/G^{(1)})]$$

vanishes. Note that this condition is satisfied if the two materials are incompressible, or trivially if they are identical. Otherwise, the near-tip asymptotic stress and deformation fields are oscillatory in nature leading to "interpenetration" of the crack faces, unless contact is enforced near the crack tip (Comminou, 1977). In spite of this difficulty, Rice (1988) has argued that these solutions provide useful information characterizing the near-tip fields in typical circumstances when the size of the interpenetration zone is small compared to the size of the crack. According to Hutchinson (1989), it is perhaps more important to note that the tensile and shear effects are coupled in the vicinity of the crack tip, making the understanding of interfacial fracture mechanics intrinsically harder than the standard fracture mechanics of homogeneous materials. The consequence in the context of our problem is that we expect difficulties in our solutions for values of α near unity when the values of β, $\nu^{(1)}$ and $\nu^{(2)}$ are such that the value of the elastic bimaterial parameter ε is different from zero.

The numerical integration of eqns (21) was carried out by means of the same scheme used in the anti-plane strain problem. In order to get started, we provide the values of s and γ, thus determining the values of $\mathbf{y}(0+)$, $\mathbf{y}'(0+)$ for given values of α, β, $\nu^{(1)}$ $\nu^{(2)}$. We then integrate eqns (21) to determine $\mathbf{y}(\theta)$ for $0 < \theta \leqslant \pi$. Given the values of $y_1(\pi)$ and $y_3(\pi)$, we check to see whether they vanish, and iterate in our guesses for s *and* γ until convergence is achieved. Finally, we renormalize our solutions such that $y_2(\theta_1) = 1$. Note that the determination of $\mathbf{y}'(0+)$ requires special numerical treatment, and also that y_3 and y_4 are well-behaved near $\theta = \pi$, so that even though (21) is ill-conditioned at $\theta = \pi$, a procedure analogous to that used in the anti-plane strain case can be applied here also.

3.2. *Linear-hardening results*

Whenever the values of β, $\nu^{(1)}$ and $\nu^{(2)}$ are such that the elastic bimaterial parameter ε vanishes, there are two solutions to the above eigenvalue problem for all values of α such that $0 < \alpha \leqslant 1$; one corresponding to a tensile-like solution with values of the mixity parameter m_{pl} close to unity, and the other corresponding to a shear-like solution with values of the mixity parameter m_{pl} close to zero. On the other hand, whenever the values of β, $\nu^{(1)}$ and $\nu^{(2)}$ are such that the elastic bimaterial parameter ε is different from zero, there exist two initially distinct solutions for small enough values of α, which coalesce at a sufficiently large critical value of the hardening parameter, $\alpha_c < 1$. In this case no solutions were found for values of α greater than α_c. As was noted above, this is consistent with the lack of existence of variable-separable solutions in the elastic problem ($\alpha = 1$) when ε is different from zero. Also note that the lack of existence of variable-separable solutions does not preclude the existence of other more general solutions, which could be detected by the numerical analysis of Part II.

The specific results of this section are presented in Figs 4–10 and in Tables 2–5. Figures 4 show plots of the singularity strengths as functions of the hardening for different values of β, $\nu^{(1)}$ and $\nu^{(2)}$. Figure 4a shows results for the case where the elastic bimaterial parameter is zero so that the elastic limit is well-defined. Results are given for a sequence of values of $\beta = 0$, 0.5 and 1, for $\nu^{(1)} = \nu^{(2)} = 0.5$, and also for $\beta = 0$ and $\nu^{(1)} = \nu^{(2)} = 0.3$. For each such combination of the material parameters, there are two curves: one corresponding to the "shear" solution, which has positive curvature, and the other corresponding to the "tensile" solution, which changes curvature at an intermediate value of the hardening. Note also the cross-over behavior of the two solutions. Thus for a fixed value of β, the singularity is stronger in the tensile solution for large hardening, but it is weaker for small hardening. We can also see that s is stronger for larger values of β, and stronger for larger values of ν.

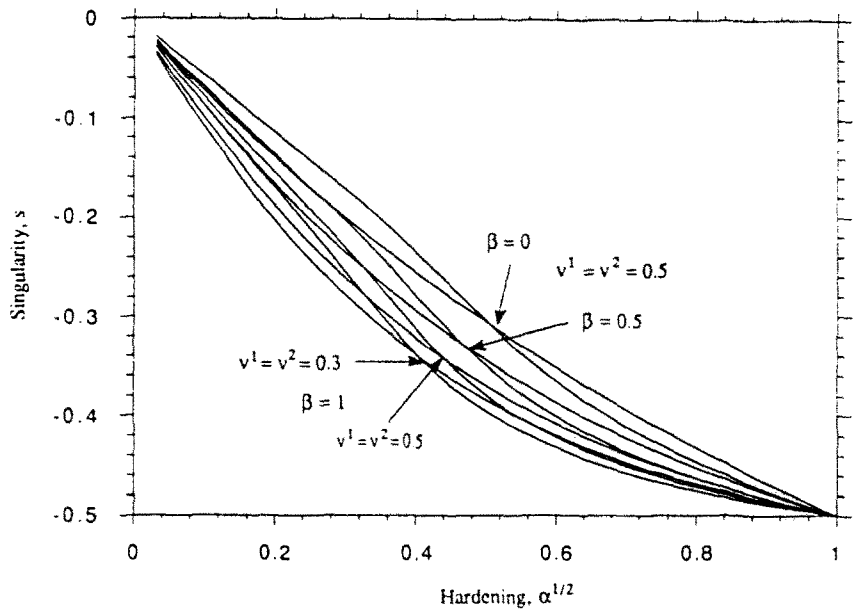

Fig. 4a. Strength of the singularity as a function of hardening in plane strain for the "tensile" and "shear" sets of solutions for four different cases when the bimaterial elastic parameter $\varepsilon = 0$. Each set of curves crosses over at some intermediate value of the hardening parameter, with the "tensile" curve lying above the "shear" curve for small hardening, and below it for large hardening.

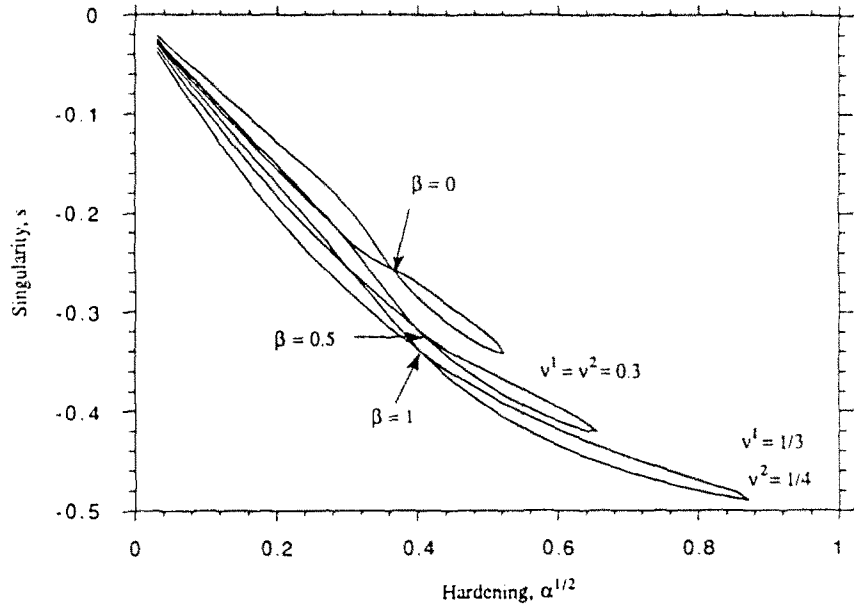

Fig. 4b. Strength of the singularity as a function of hardening in plane strain for the "tensile" and "shear" sets of solutions for three different cases when the bimaterial elastic parameter $\varepsilon \neq 0$. Each set of curves crosses over at some intermediate value of the hardening parameter, and coalesce at some maximum critical value of the hardening. For each set, the "tensile" curve lies above the "shear" curve for small hardening, and below it for large hardening.

Figure 4b shows results for three cases when $\varepsilon \neq 0$, corresponding to two cases with values of $\beta \neq 1$ (0 and 0.5) and $\nu^{(1)} = \nu^{(2)} = 0.3$, and one case for which $\beta = 1$, but $\nu^{(1)} = 1/3 \neq \nu^{(2)} = 1/4$. As anticipated in the previous subsection, no solutions were found for values of α close to unity (the elastic limit), but two solutions exist for sufficiently small values of α. These two solutions, which initially have a behavior that is similar to the zero-

Table 2a. Strength of the singularity, mode mixity, unloading and reloading angles versus hardening in plane strain for the "tensile" solution ($\beta = 1$, $\nu^{(1)} = \nu^{(2)} = 0.5$)

α	s	γ	θ_3	θ_4	θ_1	θ_2
0.9	−0.49393	−0.46793	16.407	50.857	115.94	
0.8	−0.48669	−0.49471	16.483	52.131	116.09	
0.7	−0.47786	−0.52451	16.484	53.537	116.32	
0.6	−0.46679	−0.5579	16.371	55.057	116.7	
0.5	−0.45236	−0.59564	16.069	56.621	117.31	
0.4	−0.43245	−0.63882	15.429	58.001	118.39	
0.3	−0.40225	−0.68911	14.071	58.329	120.4	
0.2	−0.34811	−0.75078	10.719	52.96	124.2	178.94
0.1	−0.2434	−0.89432	3.969	24.247	128.62	167.48
0.05	−0.17203	−1.0453	0.731	3.891	131.07	158.55
0.03	−0.13572	−1.1102			130.88	155.98
0.01	−0.08024	−1.2171			129.78	153.26
0.005	−0.05719	−1.2661			129.14	152.37
0.001	−0.0258	−1.3365			127.94	151.37

Table 2b. Strength of the singularity, mode mixity, unloading and reloading angles versus hardening in plane strain for the "shear" solution ($\beta = 1$, $\nu^{(1)} = \nu^{(2)} = 0.5$)

α	s	γ	θ_1	θ_2
0.9	−0.49178	1.4072	43.52	
0.8	−0.48229	1.3767	43.171	
0.7	−0.47112	1.3406	42.827	
0.6	−0.45764	1.2967	42.475	
0.5	−0.44087	1.2419	42.089	
0.4	−0.41919	1.1709	41.623	
0.3	−0.38964	1.074	40.979	
0.2	−0.3461	0.93168	39.925	
0.1	−0.27223	0.69177	37.712	
0.05	−0.20648	0.48066	35.182	
0.03	−0.16578	0.35139	33.283	
0.01	−0.10061	0.14737	29.504	179.99
0.005	−0.07259	0.06114	27.471	179.98
0.001	−0.03343	−0.0569	23.882	179.95

ε case (including the cross-over behavior), eventually coalesce at some critical value of the hardening α_c, smaller than unity. The value of α at which the coalescence of the solutions takes place is smaller the larger the value of ε. In our sample results, the three values of α_c, 0.2740, 0.4279 and 0.7595, correspond to the three values of ε, 0.9355, 0.0305 and −0.01875. In all cases, s is proportional to $-\alpha^{1/2}$ as $\alpha \to 0$, suggesting the possibility of existence of solutions when the ductile material is perfectly plastic. By comparison to the results of Ponte Castañeda (1987a) for the propagating crack in the homogeneous linear-hardening material, we find that the singularity is in general stronger for the interfacial crack, except for very small values of α, when the tensile homogeneous solution is found to be anomalous in that s does not approach zero as α approaches zero.

Figures 5 depict the corresponding results for the mixity parameter m_{pl} as functions of α for the same combination of choices of β, $\nu^{(1)}$ and $\nu^{(2)}$. Figure 5a gives results for the case when the combination of elastic parameters is such that $\varepsilon = 0$. We find that one of the solutions shows values of m_{pl} close to unity, and the other has values of m_{pl} close to zero. This provides justification for our usage of the "tensile" and "shear" denominations for the two solutions, respectively, although they are not strictly mode I or mode II solutions. More specifically, the tensile solution is found to have mixity slightly larger than unity for larger hardening, and smaller than unity for small hardening (this means that the in-plane shear stress on the interfacial line changes sign at some intermediate value of α), and the results show moderate dependence on the other parameters. The shear solution has mixity

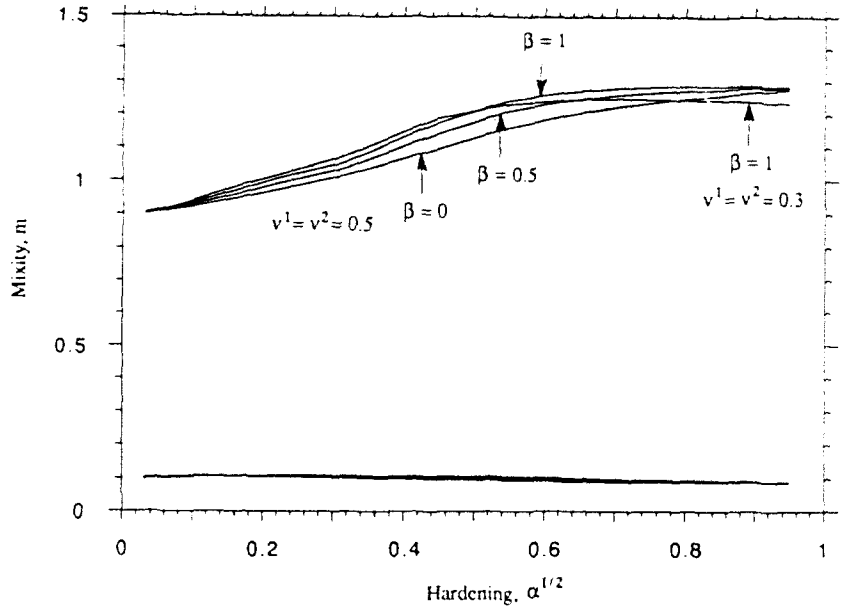

Fig. 5a. Mode mixity as a function of hardening for the set of "tensile" and "shear" solutions corresponding to the four different cases when the bimaterial elastic parameter $\varepsilon = 0$. The "tensile" solutions correspond to values of the mixity parameter near "1" and the "shear" solutions to values of the mixity near "0".

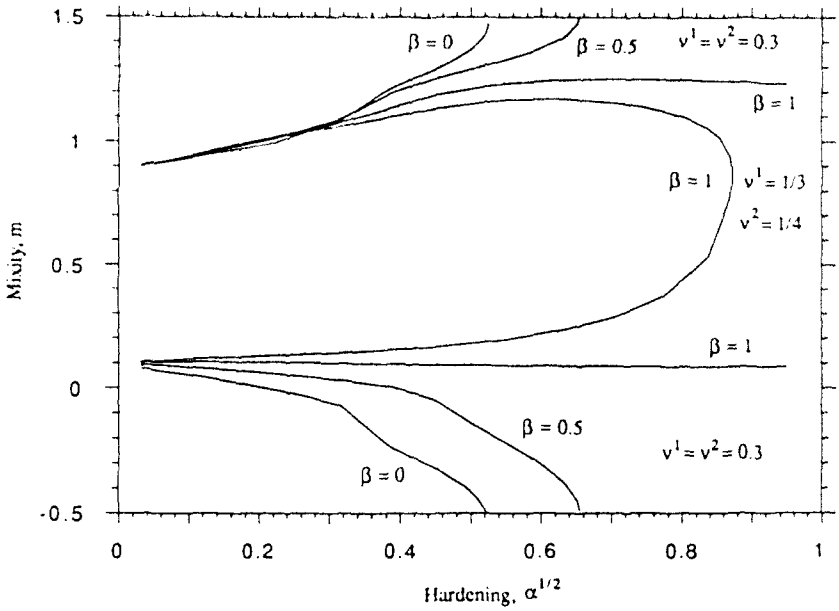

Fig. 5b. Mode mixity as a function of hardening for the set of "tensile" and "shear" solutions corresponding to the three different cases when the bimaterial elastic parameter $\varepsilon \neq 0$. In addition, a "model" solution is shown for the case when $\varepsilon = 0$; this set of solutions is easily identified because (unlike the $\varepsilon \neq 0$ solutions) the "tensile" and "shear" solutions do not coalesce for any values of the hardening parameter.

very close to 0.1 for all values of α, and shows very little variation with the other parameters. Note that in this case (when $\varepsilon = 0$), the fact that the mixities are distinct for the two solutions shows that the solutions are indeed distinct even for values of α when the values of s happen to coincide (this occurs for $\alpha = 1$ and in the limit as $\alpha \to 0$, as well as when the two solutions for s cross over). Figure 5b gives the corresponding results for the cases when

Table 3a. Strength of the singularity, mode mixity, unloading and reloading angles versus hardening in plane strain for the "tensile" solution ($\beta = 0$, $\nu^{(1)} = \nu^{(2)} = 0.5$)

α	s	γ	θ_3	θ_4	θ_1	θ_2
0.9	−0.48806	−0.47126	15.964	50.003	115.6	
0.8	−0.47427	−0.50226	15.579	50.273	115.38	
0.7	−0.45802	−0.53768	15.098	50.495	115.24	
0.6	−0.43838	−0.57894	14.479	50.605	115.22	
0.5	−0.4138	−0.6283	13.638	50.463	115.46	
0.4	−0.38146	−0.6896	12.408	49.72	116.2	
0.3	−0.33584	−0.77005	10.392	47.327	118.04	180
0.2	−0.26726	−0.87976	6.564	38.977	121.81	177.63
0.1	−0.18071	−1.0309	1.346	13.426	126.24	168.25
0.05	−0.1284	−1.1273			126.42	163.94
0.03	−0.09981	−1.1817			125.85	162.24
0.01	−0.05794	−1.2671			124.56	160.09
0.005	−0.04106	−1.3036			123.79	159.33
0.001	−0.01842	−1.3543			122.31	158.42

Table 3b. Strength of the singularity, mode mixity, unloading and reloading angles versus hardening in plane strain for the "shear" solution ($\beta = 0$, $\nu^{(1)} = \nu^{(2)} = 0.5$)

α	s	γ	θ_1	θ_2
0.9	−0.48383	1.379	43.507	
0.8	−0.46589	1.3188	43.071	
0.7	−0.44579	1.2517	42.557	
0.6	−0.423	1.176	41.943	
0.5	−0.39671	1.089	41.191	
0.4	−0.36572	0.98722	40.24	
0.3	−0.32796	0.86408	38.979	
0.2	−0.27935	0.70719	37.171	
0.1	−0.20926	0.4844	34.119	
0.05	−0.15462	0.31403	31.26	180
0.03	−0.12292	0.21679	29.337	180
0.01	−0.07408	0.06988	25.811	179.97
0.005	−0.05345	0.00929	24.008	179.96
0.001	−0.02472	−0.07272	20.898	179.92

the combination of parameters is such that ε does not vanish (and also for comparison for one case when it does vanish). In this picture, it is clearly observed that the two solutions, which are initially (for small α) distinct with mixities near zero and unity, eventually coalesce at the critical value of $\alpha = \alpha_c$, reaching the same value for their mixities. This is clearly seen for the case when $\beta = 1$ and the values of ν are different. To deduce the same conclusion for the cases when the values of ν are the same, but $\beta \neq 1$, we need to take into account the periodicity of the mixity, and note that for these two other cases the solutions meet at the next branch of the solution. Also note that values of the mixity in the range from zero to unity (unity to two) correspond to positive (negative) shear stress in the interfacial line ahead of the crack. Therefore, the coalescent solutions can either have positive or negative shear stresses in the interfacial line ahead of the crack, depending on whether ε is negative or positive, respectively.

Tables 2–5 give more detailed results for the resulting values of the singularity strength s, the mixity angle γ, and the unloading and reloading angles θ_1 and θ_2 for the tensile and shear solutions as function of the hardening parameter α for some of the above mentioned choices for β, $\nu^{(1)}$ and $\nu^{(2)}$. In general, the width of the plastic loading sectors is larger for the tensile solution than for the shear solution, particularly for the smaller values of α. For the larger values of α, and mainly for the tensile solutions (and some shear coalescing solutions), four and five sector (with alternating plastic loading and elastic unloading sectors) solutions are observed that are reminiscent of the solutions observed by Ponte Castañeda (1987a) for the antisymmetric growing cracks in the homogeneous linear-hardening material. We recall that this is due to the fact that, because $y_c(\theta)$ may have two peaks,

Table 4a. Strength of the singularity, mode mixity, unloading and reloading angles versus hardening in plane strain for the "tensile" solution ($\beta = 0$, $\nu^{(1)} = \nu^{(2)} = 0.3$)

α	s	γ	θ_3	θ_4	θ_1	θ_2
0.27396	−0.34108	−1.2429	36.831	41.299	117.32	
0.2739	−0.34147	−1.2318			117.16	
0.273	−0.34216	−1.2048			116.76	
0.27	−0.34234	−1.1705			116.23	
0.25	−0.33723	−1.0912			114.92	
0.2	−0.31366	−1.0378			114.66	
0.1	−0.20769	−1.0466			126.71	171.51
0.05	−0.1429	−1.1126			130.53	161.96
0.03	−0.11149	−1.1674			129.82	160.07
0.01	−0.06488	−1.2557			127.92	158.12
0.005	−0.04601	−1.2944			126.81	157.56
0.001	−0.02066	−1.3495			124.75	157

Table 4b. Strength of the singularity, mode mixity, unloading and reloading angles versus hardening in plane strain for the "shear" solution ($\beta = 0$, $\nu^{(1)} = \nu^{(2)} = 0.3$)

α	s	γ	θ_1	θ_3	θ_4	θ_2
0.27396	−0.34108	1.8987	36.831	41.299	117.32	
0.2739	−0.34073	1.8902	36.341	43.067	117.44	
0.273	−0.33926	1.8597	33.555	47.366	117.86	
0.27	−0.33649	1.8148	35.105	52.058	118.44	
0.25	−0.32367	1.6655	34.747	63.887	120.11	
0.2	−0.29525	1.4242	34.491	79.329	122.24	
0.1	−0.23625	0.84931	33.851	125.9	129.22	
0.05	−0.17223	0.55094	31.574			180
0.03	−0.13632	0.39666	29.8			180
0.01	−0.0819	0.17371	26.325			179.97
0.005	−0.05909	0.08369	24.476			179.95
0.001	−0.02736	−0.03773	21.193			179.9

two additional regions may appear and the two angles θ_3 and θ_4 may be required to describe the start of the new reloading zone and the new unloading zone, respectively. The two angles θ_1 and θ_2 retain their old meanings; they are primary in the sense that they remain in existence for small values of α.

Figures 6–10 give the angular variations (fixed r) of the stress and velocity fields for the tensile and shear solutions in the vicinity of the crack tip for a few special choices of the material parameters α, β, $\nu^{(1)}$ and $\nu^{(2)}$. Figures 6a and b correspond, respectively, to the tensile and shear solutions for the stress fields of an aluminum/alumina composite with typical values for the material parameters of $\alpha = 0.1$, $\beta = 0.2$, $\nu^{(1)} = 1/3$ and $\nu^{(2)} = 1/4$ ($\varepsilon = 0.045786$). The associated values of s and m_{pl} are -0.218488 and 1.075537, and -0.24519 and 0.00984, respectively. Figures 7a and b give the corresponding results for two coalescing solutions: the first one corresponds to a critical value of $\alpha = 0.75947$, and values of $\beta = 1$, $\nu^{(1)} = 1/3$ and $\nu^{(2)} = 1/4$ ($\varepsilon = -0.01875$), and the second one to a critical value of $\alpha = 0.27396$, and values of $\beta = 0$, $\nu^{(1)} = \nu^{(2)} = 0.3$ ($\varepsilon = 0.9355$). It can be seen that, whereas the previous set of results can be identified with a tensile- and a shear-like solution, these fields are fully mixed, and quite different in nature (for example, in Fig. 7b the shear stress in the interfacial line is very large and negative in sign). Figures 8a and b give the stress distributions for the tensile and shear solutions corresponding to a very small value of the hardening, $\alpha = 0.001$, for $\beta = 0$ and $\nu^{(1)} = \nu^{(2)} = 1/2$. The striking feature of Fig. 8a is the extremely large level of triaxiality (more than 3 times the yield stress in tension) on the interfacial line, in addition to a moderate level of the shear stress, and it is vaguely reminiscent of the mode I Prandtl-like solution of Drugan *et al.* (1982) (without the constant-stress sector ahead of the crack, but instead with a centered-fan sector starting right at the interface). On the other hand, the shear solution has a dominant, but small level of shear stress in the interfacial line, and the distribution of the stresses is reminiscent of the mode II solution of Slepyan (1974) for the homogeneous perfectly plastic material.

Table 5a. Strength of the singularity, mode mixity, unloading and reloading angles versus hardening in plane strain for the "tensile" solution ($\beta = 1$, $\nu^{(1)} = 1/3$, $\nu^{(2)} = 1/4$)

α	s	γ	θ_3	θ_4	θ_1	θ_2
0.75945	−0.48938	0.18945			74.014	
0.7594	−0.48958	0.16287			75.85	
0.759	−0.48972	0.139			77.587	
0.755	−0.48981	0.06616			83.361	
0.7	−0.48588	−0.13013			99.964	
0.6	−0.47615	−0.26529			109.08	
0.5	−0.4629	−0.36028			113.92	
0.4	−0.44423	−0.44427	19.036	24.017	117.53	
0.3	−0.41607	−0.5266	16.556	28.522	120.9	
0.2	−0.36767	−0.62375			125.57	179.77
0.1	−0.26839	−0.81925			128.57	170.85
0.05	−0.18855	−1.0045			131.62	160.53
0.03	−0.1489	−1.0846			132.05	156.54
0.01	−0.08865	−1.1987			130.89	153.24
0.005	−0.06332	−1.2521			130.19	152.13
0.001	−0.02863	−1.3298			128.89	150.87

Table 5b. Strength of the singularity, mode mixity, unloading and reloading angles versus hardening in plane strain for the "shear" solution ($\beta = 1$, $\nu^{(1)} = 1/3$, $\nu^{(2)} = 1/4$)

α	s	γ	θ_1	θ_2
0.75945	−0.48938	0.18945	74.014	
0.7594	−0.480932	0.19656	73.541	
0.759	−0.48906	0.22301	71.848	
0.755	−0.48776	0.31926	65.511	
0.7	−0.47816	0.66769	54.222	
0.6	−0.46385	0.86965	49.155	
0.5	−0.44795	0.95016	46.721	
0.4	−0.42807	0.9732	45.023	
0.3	−0.40107	0.9499	43.548	
0.2	−0.36057	0.86929	41.913	
0.1	−0.28898	0.68145	39.286	
0.05	−0.22225	0.48946	36.544	
0.03	−0.17972	0.36444	34.53	180
0.01	−0.11008	0.15943	30.487	180
0.005	−0.07968	0.07078	28.294	179.98
0.001	−0.03685	−0.05179	24.389	179.95

Finally, Figs 10 give the velocity distributions for the tensile and shear solutions corresponding to a small value of the hardening parameter ($\alpha = 0.001$), and two values of β (0 and 1). It is seen that, even though s is small, the choice of the radial dependence for the velocity (r^s/s) leads to bounded variations for the angular dependence of the fields.

3.3. *Formulation of the perfectly plastic problem*

In this section, we deal with the same interfacial growing crack problem as in the previous section with the difference that the plastic behavior of the material in the upper half will be taken perfectly-plastic of the Mises-type instead of linear hardening. Thus, the same equilibrium equations (17) and (18) apply, and the stress-strain relation takes the form of (19), where now $\dot{\Lambda} \geqslant 0$ is an undetermined scalar function for active plastic loading, that vanishes for elastic unloading. Hence, in the regions of active plastic response, the governing equations must be supplemented by the Mises yield condition

$$\sigma_e = [(3/2)\mathbf{S}:\mathbf{S}]^{1/2} = \sqrt{3}\tau_0, \tag{30}$$

where $\mathbf{S}$ is the stress deviator, and τ_0 is the yield stress in shear.

Rice (1982) has shown that these governing equations admit only four types of asymptotic solutions with bounded stresses and logarithmic velocities. Thus, in the vicinity of the

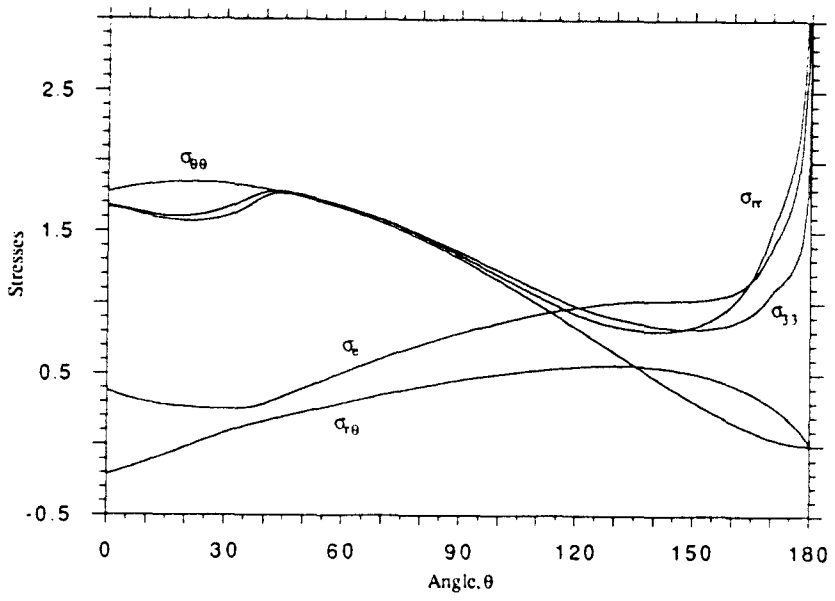

Fig. 6a. Angular variations of the "tensile" stress fields in plane strain for aluminum/alumina ($\alpha = 0.1$, $\beta = 0.2$, $\nu^{(1)} = 1/3$, $\nu^{(2)} = 1/4$).

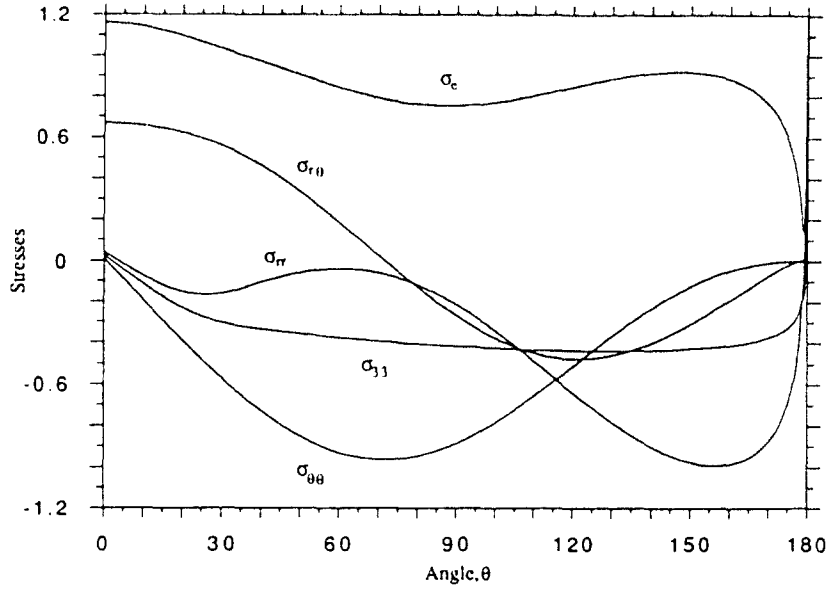

Fig. 6b. Angular variations of the "shear" stress fields in plane strain for aluminum/alumina ($\alpha = 0.1$, $\beta = 0.2$, $\nu^{(1)} = 1/3$, $\nu^{(2)} = 1/4$).

crack tip, we can only have four types of sectors meeting along radial lines emanating from the crack tip: singular plastic sectors of either the constant-stress or centered-fan type, non-singular plastic sectors and elastic sectors. The stress and velocity fields in each of these sectors (with the exception of the non-singular plastic sectors) can be found explicitly. The resulting fields need to be connected across the straight boundaries separating them. Drugan and Rice (1984) have shown that all the components of the stress must be continuous across such quasi-statically propagating boundaries. Additionally, they have shown that, except under exceptional circumstances, the velocity fields must also be continuous. Here, we will look for solutions with continuous velocity fields.

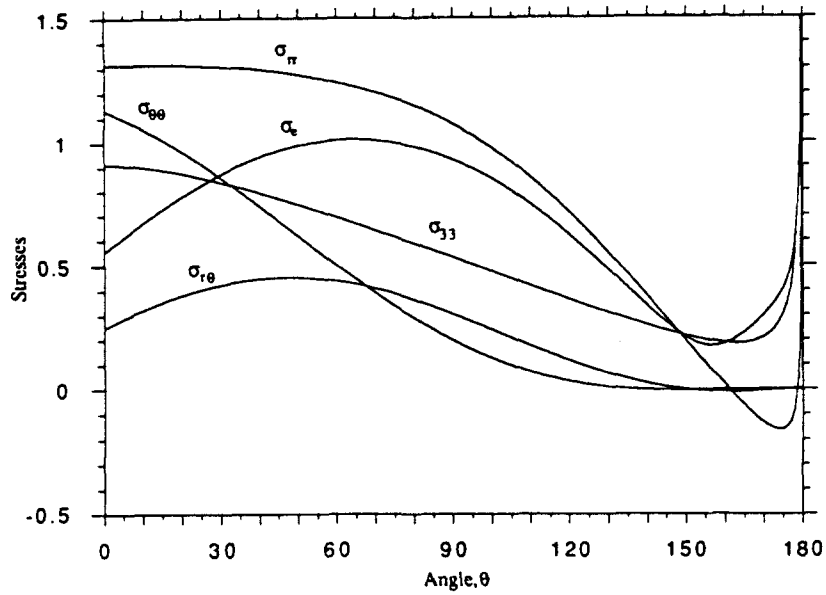

Fig. 7a. Angular variations of the stress fields for a "coalescing" solution in plane strain ($\alpha = 0.75947$, $\beta = 1$, $\nu^{(1)} = 1/3$, $\nu^{(2)} = 1/4$, $\varepsilon = -0.01875$).

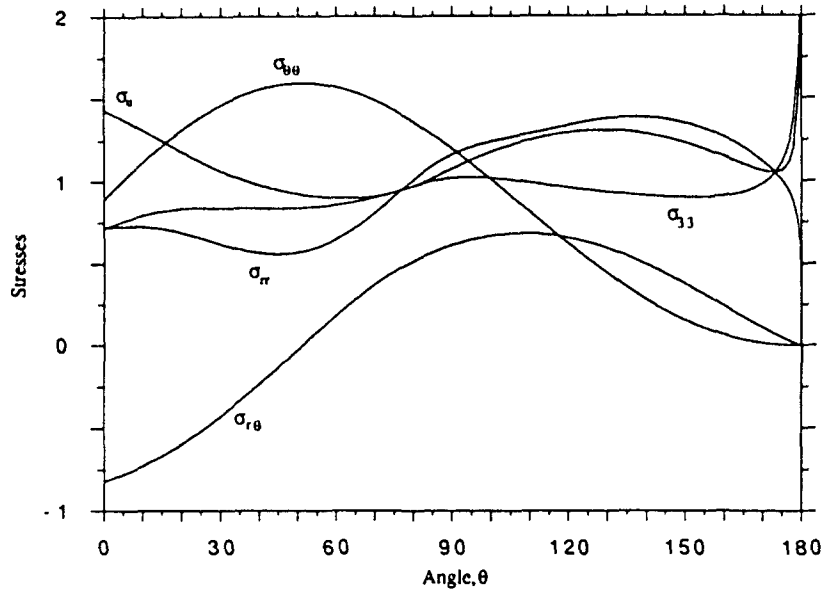

Fig. 7b. Angular variations of the stress fields for a "coalescing" solution in plane strain ($\alpha = 0.27396$, $\beta = 0$, $\nu^{(1)} = \nu^{(2)} = 0.3$, $\varepsilon = 0.9355$).

The fields can also be determined explicitly for the brittle material on the lower half, but, for simplicity, in this work we will assume that the brittle material is rigid. This will obviate the need to solve for the fields in the lower half, and therefore simplify the analysis considerably.

It follows that the appropriate boundary conditions for this problem are the traction-free condition on the upper crack face, requiring that

$$\sigma_{r\theta}(r, \pi) = \sigma_{\theta\theta}(r, \pi) = 0, \tag{31}$$

and the condition of continuity of the velocities on the interfacial line ahead of the crack,

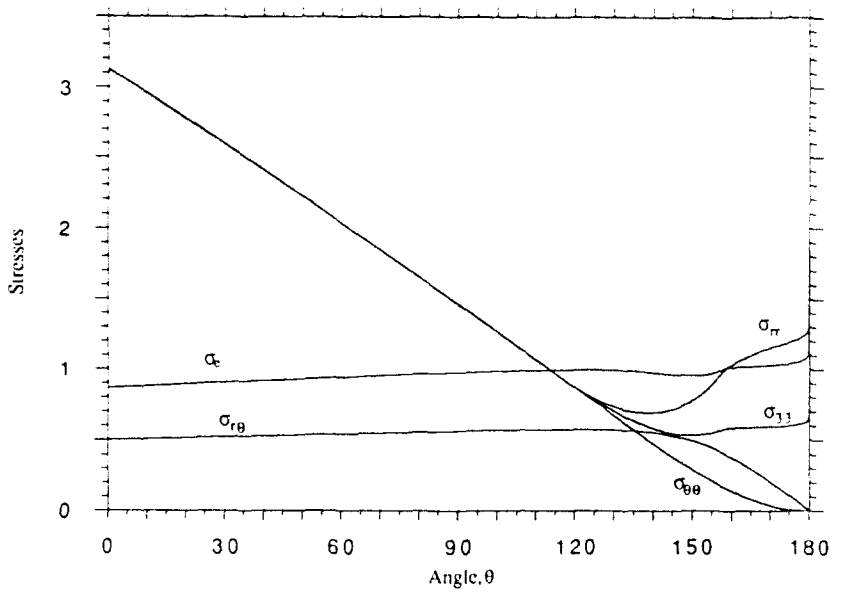

Fig. 8a. Angular variations of the "tensile" stress fields in plane strain for small hardening ($\alpha = 0.001$, $\beta = 0$, $\nu^{(1)} = \nu^{(2)} = 0.5$).

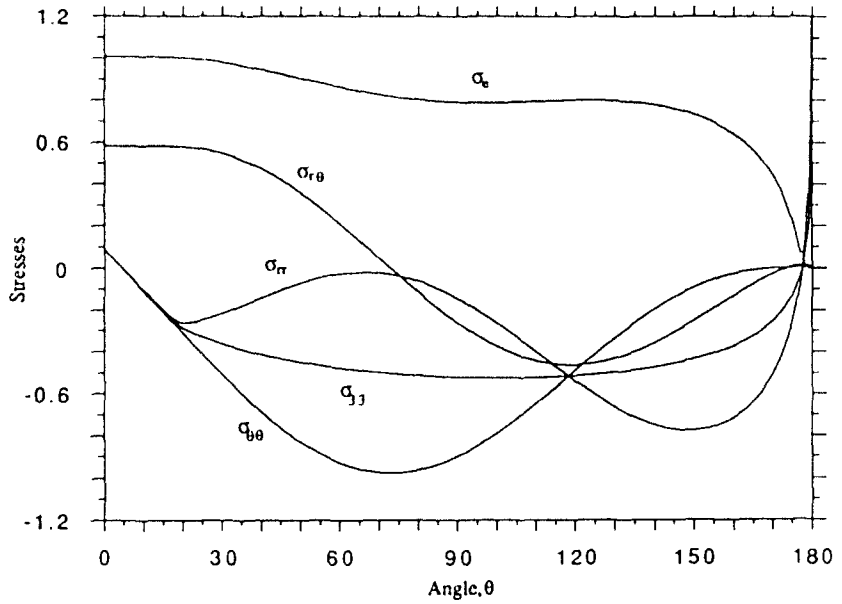

Fig. 8b. Angular variations of the "shear" stress fields in plane strain for small hardening ($\alpha = 0.001$, $\beta = 0$, $\nu^{(1)} = \nu^{(2)} = 0.5$).

requiring in turn that

$$v_r(r, 0) = v_\theta(r, 0) = 0. \tag{32}$$

The condition of continuity of tractions serves only to determine the stress level on the lower half of the interface.

3.4. *Perfectly-plastic results*

Anticipating that the perfectly-plastic results will be related to the results obtained in the previous section for small hardening, we seek solutions for the perfectly-plastic problem

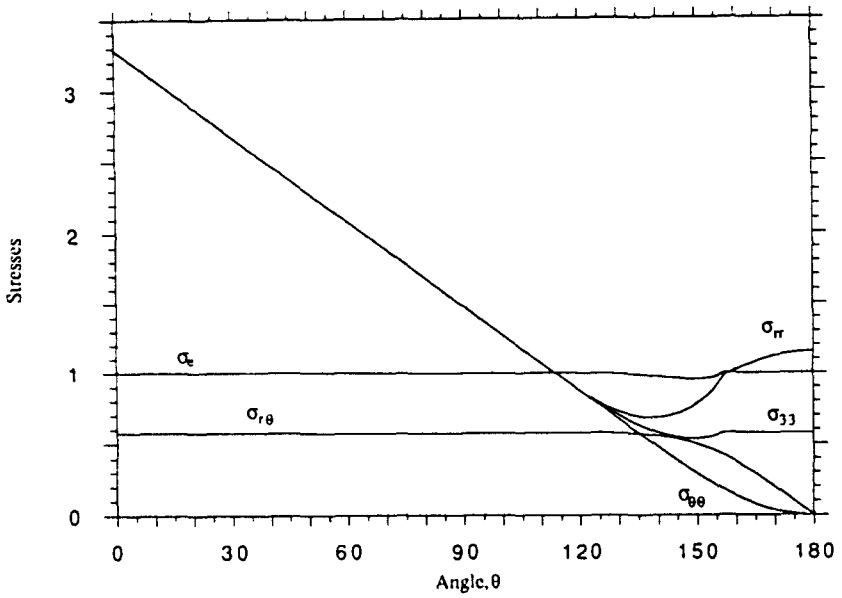

Fig. 9a. Angular variations of the "tensile" stress fields in plane strain for perfect plasticity ($\alpha = 0$, $\beta = 0$, $\nu^{(1)} = \nu^{(2)} = 0.5$).

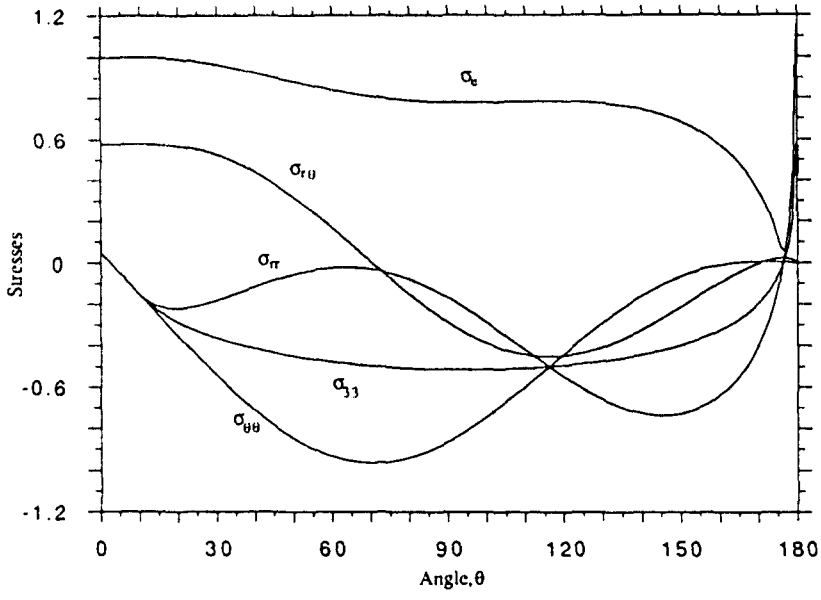

Fig. 9b. Angular variations of the "shear" stress fields in plane strain for perfect plasticity ($\alpha = 0$, $\beta = 0$, $\nu^{(1)} = \nu^{(2)} = 0.5$).

having a centered-fan sector ahead of the crack ($0 < \theta < \theta_1$), followed by an elastic unloading sector ($\theta_1 < \theta < \theta_2$), and then by a constant-stress sector extending to the upper crack face ($\theta_2 < \theta < \pi$), that in addition satisfy the boundary conditions (31) and (32). For simplicity, we will only consider here the case when the ductile material is incompressible ($\nu^{(1)} = 1/2$), which results in $\sigma_{33} = (\sigma_{rr} + \sigma_{\theta\theta})/2$. Then, making use of the results of Rice (1982), we have the following expressions for the stress and velocity fields in the different sectors:

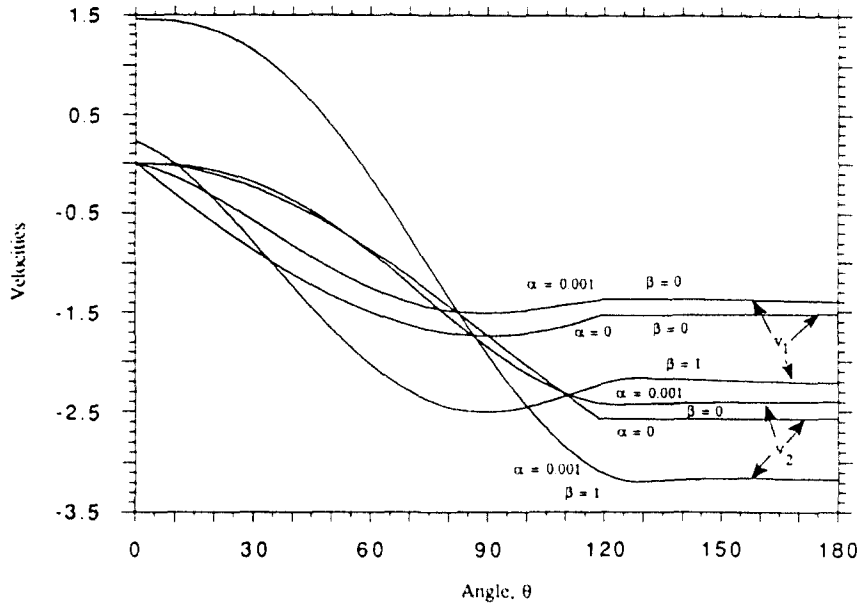

Fig. 10a. Angular variations of the "tensile" velocity fields in plane strain for small hardening and perfect plasticity ($v^{(1)} = v^{(2)} = 0.5$).

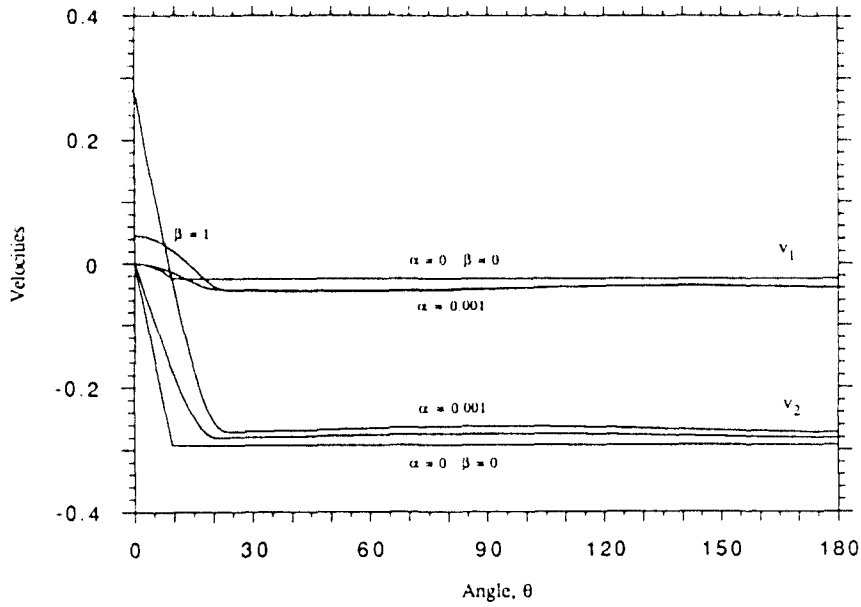

Fig. 10b. Angular variations of the "shear" velocity fields in plane strain for small hardening and perfect plasticity ($v^{(1)} = v^{(2)} = 0.5$).

(i) *Centered-fan sector*

$$\sigma_{r\theta} = \tau_0, \quad \sigma_{rr} = \sigma_{\theta\theta} = \tau_0(A - 2\theta), \tag{33}$$

$$v_r = -(5-4\nu^{(1)})(\tau_0/E^{(1)})V\sin\theta\ln(r/R),$$
$$v_\theta = (5-4\nu^{(1)})(\tau_0/E^{(1)})V(1-\cos\theta)\ln(r/R), \tag{34}$$

$$\dot{\Lambda} = -(5-4\nu^{(1)})(V/2E^{(1)})\ln(r/R)/r. \tag{35}$$

(ii) *Elastic sector*

$$\sigma_{12} = \tau_0[B_1(2\theta + \sin 2\theta) - B_2 \cos 2\theta + C_{12}],$$
$$\sigma_{11} = \tau_0[4B_1 \ln|\sin\theta| + B_1 \cos 2\theta + B_2(2\theta + \sin 2\theta) + C_{11}],$$
$$\sigma_{22} = \tau_0[-B_1 \cos 2\theta + B_2(2\theta - \sin 2\theta) + C_{22}], \tag{36}$$

$$v_1 = 4(1-\nu^{(1)2})V(\tau_0/E)B_1 \ln(r/R),$$
$$v_2 = 4(1-\nu^{(1)2})V(\tau_0/E)B_2 \ln(r/R). \tag{37}$$

(iii) *Constant-stress sector*

$$\sigma_{12} = 0, \quad \sigma_{11} = 2\tau_0, \quad \sigma_{22} = 0, \tag{38}$$

$$v_1 = 4(1-\nu^{(1)2})V(\tau_0/E)D_1 \ln(r/R),$$
$$v_2 = 4(1-\nu^{(1)2})V(\tau_0/E)D_2 \ln(r/R), \tag{39}$$

$$\dot{\Lambda} = (V/E)(D_1 \cos\theta + D_2 \sin\theta)(r\cos 2\theta)^{-1}. \tag{40}$$

Note that the boundary conditions (31) and (32) have already been imposed in the derivation of these results. Here R is a measure of the size of the plastic zone that is left undetermined by the asymptotic analysis.

These fields involve 10 unknown constants (A, B_1, B_2, C_{12}, C_{11}, C_{22}, D_1, D_2, θ_1 and θ_2), and must be subjected to continuity of the three in-plane stresses (σ_{11} is automatically continuous) and the two in-plane velocities across each of the two (unloading and reloading) boundaries for a total of 10 conditions. Two sets of solutions of this nonlinear algebraic system were found. The first set of solutions corresponds to a "tensile" solution, and is given by

$$\theta_1 \approx 118.57801^\circ, \qquad \theta_2 \approx 157.16784^\circ,$$
$$B_1 = D_1 \approx -0.878167, \quad B_2 = D_2 \approx -1.478355,$$
$$A \approx 5.696077, \qquad C_{12} \approx 3.156512,$$
$$C_{11} \approx 6.341533, \qquad C_{22} \approx 8.554228, \tag{41}$$

and the second corresponds to a "shear" solution, and is given by

$$\theta_1 \approx 9.70575^\circ, \qquad \theta_2 \approx 179.81688^\circ,$$
$$B_1 = D_1 \approx -0.168588, \quad B_2 = D_2 \approx -0.0143135,$$
$$A \approx 0.0867062, \qquad C_{12} \approx 1.042803,$$
$$C_{11} \approx -1.616376, \qquad C_{22} \approx -0.0786508. \tag{42}$$

The associated stress fields are depicted in Figs 9a and b, respectively. Note that the yield condition is nowhere violated ($\sigma_e < \sigma_0$ for $\theta_1 < \theta < \theta_2$). Also note that $\dot{\Lambda} > 0$ near the crack tip in both plastic sectors. The angular variations of the velocities are shown in Figs 10. Also, the near-tip plastic mixity factors for the two solutions are $m_{pl} = 0.88936$, and $m_{pl} = 0.05506$, respectively. It is interesting to remark that, as was the case with the anti-plane strain solutions, the angular variations of the stress and velocity fields for the linear-hardening problem appear to approach the corresponding perfectly plastic variations, provided the radial dependence of the velocities is appropriately normalized with respect to s.

4. CONCLUDING REMARKS

In Part I of this work, we have presented exact solutions to the asymptotic problem of a steadily and quasi-statically propagating two-dimensional crack along the interface between a brittle material and a linear-hardening, or perfectly-plastic, ductile material, under anti-plane and plane strain conditions.

In the case of anti-plane strain with linear-hardening behavior for the ductile phase, the analysis determines the strength of the assumed power singularity, as well as the associated angular variations of the stress and velocity fields for all values of the hardening parameter. The amplitude of these fields, or plastic stress intensity factor, is left undetermined by the asymptotic analysis. The determination of this plastic stress intensity factor under small scale yielding conditions is one of the goals of Part II of this work. In addition to these linear-hardening solutions, it was also remarked that the solution for a growing crack in a homogeneous perfectly-plastic solid of Chitaley and McClintock (1971) is also a solution for the growing interfacial crack problem when the ductile material is perfectly-plastic, and the brittle material is rigid.

In the case of plane strain with linear-hardening behavior for the ductile material, the asymptotic analysis not only determines the strength of the singularity and the angular variations of the fields, but also, surprisingly [this is by contrast to the mixed-mode stationary crack solutions of Shih (1974)], the "mixity" of the near-tip fields. Thus, it is found that two distinct solutions exist with slightly differing singularity strengths, and distinct, but determinate, mixities on the interfacial line ahead of the crack. For small enough hardening, one of the solutions corresponds to a tensile-like mode, whereas the other solution corresponds to a shear-like mode. These two solutions coalesce at an intermediate critical level of the hardening, if a certain bimaterial parameter is not zero. In this case, no variable separable solutions are found for values of the hardening parameter larger than the critical level. On the other hand, if the bimaterial parameter vanishes, the two solutions remain distinct for all values of the hardening parameter up to the perfectly-elastic limit. As we have seen, this picture is consistent with the fact that no variable separable solutions exist for the corresponding linear-elastic problem when the bimaterial parameter is nonzero. In addition to these *linear-hardening* solutions, we have also found two similar solutions for the corresponding plane strain problem with a *perfectly-plastic* ductile material bonded to a rigid brittle material. These solutions are fully continuous, and are consistent with the small-hardening results, depicting fixed mixities at the crack tip that correspond to a tensile- and a shear-like solution. The numerical analyses of Part II will determine what role, if any, the asymptotic solutions play in the full solution of the corresponding interfacial small scale yielding problems, and if applicable, it will determine the corresponding plastic stress intensity factors, and analyze their dependence on the applied elastic stress intensity factors (and their mixity).

It is important to note that the prediction of *discrete* and *determinate* asymptotic mixities at the crack tip does *not* seem to be an artifact of the *interfacial* nature of the problem, but instead of the quasi-static *crack growth* feature. Ponte Castañeda and Bose (1990) have made parallel observations for crack growth in a homogeneous linear-hardening material. Furthermore, as the linear-hardening and perfectly plastic interfacial growing crack solutions developed here show, this phenomenon of fixed mixities at the crack tip does *not* seem to be dependent on the specific *constitutive* model for the ductile material, *nor* on the *variable-separable* nature of the linear-hardening solutions (the perfectly-plastic solutions are not variable-separable!). It is also worth mentioning that even if linear-hardening is not an accurate model for the plastic behavior of ductile materials at large strains, the linear-hardening solutions derived in this work could at the very least be interpreted as a useful interpolation between the two limiting cases corresponding to perfectly-elastic and perfectly-plastic behavior for the ductile phase. Since the essential feature of stable crack growth is the dissipation of energy via the production of residual plastic strains in the wake of the crack, it can be argued that the role played by hardening in this phenomenon is more important than the *specific* model of hardening selected. Given the well-known difficulties associated with near-tip asymptotic analysis of growing cracks with other hardening models, the choice of a linear-hardening model in this work should

be amply justified. Perhaps a more critical issue would be the inclusion of finite kinematics, if the goal of the analysis is to predict accurately the fields very close to the tip of the crack. Lastly, in the context of application to practical problems, the asymptotic solutions obtained in this part of the work correspond to the most singular term in an expansion that may include other terms in order to ensure satisfaction of the appropriate conditions on the boundary of the specimen. For this reason, the significance of these asymptotic solutions should be viewed in the context of a larger scheme including numerical solutions of the type carried out in Part II.

Acknowledgements—This part of the work was supported by a Research Initiation grant from the National Science Foundation (MSM-8809177). One of the authors (P. Ponte Castañeda) is grateful to Mr K. Bose of The Johns Hopkins University for his valuable assistance with some of the numerical computations.

REFERENCES

Amazigo, J. C. and Hutchinson, J. W. (1977). Crack-tip fields in steady crack growth with linear strain-hardening. *J. Mech. Phys. Solids* **25**, 81–97.

Chitaley, A. D. and McClintock, F. A. (1971). Elastic-plastic mechanics of steady crack growth under anti-plane shear. *J. Mech. Phys. Solids* **19**, 147–163.

Comninou, M. (1977). The interface crack. *J. Appl. Mech.* **44**, 631–636.

Dean, R. H. and Hutchinson, J. W. (1980). Quasi-static steady crack growth in small-scale yielding. In *Fracture Mechanics: Twelfth Conf. ASTM STP* 700, pp. 383–405, Philadelphia.

Drugan, W. J. and Rice, J. R. (1984). Restrictions on quasi-statically moving surfaces of strong discontinuity in elastic-plastic solids. In *Mechanics of Material Behavior* (Edited by G. J. Dvorak and R. T. Shield), pp. 59–73. Elsevier, Amsterdam.

Drugan, W. J., Rice, J. R. and Sham, T. L. (1982). Asymptotic analysis of growing plane strain tensile cracks in elastic ideally plastic solids. *J. Mech. Phys. Solids* **30**, 447–473.

England, A. H. (1965). A crack between dissimilar media. *J. Appl. Mech.* **32**, 400–402.

Erdogan, F. (1965). Stress distribution in bonded dissimilar materials with cracks. *J. Appl. Mech.* **32**, 403–410.

Gao, Y.-C. (1980). Elastic-plastic field at the tip of a crack growing steadily in perfectly plastic medium (in Chinese). *Acta Mech. Sin.* **1**, 48–56.

Green, G. and Knott, J. F. (1975). On effects of thickness on ductile crack growth in mild steel. *J. Mech. Phys. Solids* **23**, 167–183.

Hutchinson, J. W. (1989). Mixed mode fracture mechanics of interfaces. Technical report MECH-139, Division of Applied Sciences, Harvard University.

Hutchinson, J. W., Mear, M. E. and Rice, J. R. (1987). Crack paralleling an interface between dissimilar materials. *J. Appl. Mech.* **54**, 828–832.

Knowles, J. K. and Sternberg, E. (1983). Large deformation near a tip of an interface crack between two Neo-Hookean sheets. *J. Elasticity* **13**, 405–421.

Narasimham, R., Rosakis, A. J. and Hall, J. F. (1987). A finite element study of stable crack growth under plane stress conditions: Part I—Elastic-perfectly plastic solids. *J. Appl. Mech.* **54**, 838–845.

Parks, D. M., Lam, P. S. and McMeeking, R. M. (1981). Some effects of inelastic constitutive models on crack tip fields in steady quasi-static growth. In *Advances in Fracture Research, ICF5* (Edited by D. Francois *et al.*), Vol. 5, pp. 2607–2614. Pergamon Press, Oxford.

Parks, D. M. and Zywicz, E. (1989). Elastic/perfectly-plastic small scale yielding at bimaterial interfaces. In *Advances in Fracture Research, ICF7* (Edited by K. Salama *et al.*), Vol. 4, pp. 3081–3088. Pergamon Press, Oxford.

Ponte Castañeda, P. (1986). Asymptotic fields of a perfectly-plastic, plane-stress mode II growing crack. *J. Appl. Mech.* **53**, 831–833.

Ponte Castañeda, P. (1987a). Asymptotic fields in steady crack growth with linear strain-hardening. *J. Mech. Phys. Solids* **35**, 227–268.

Ponte Castañeda, P. (1987b). Plastic stress intensity factors in steady crack growth. *J. Appl. Mech.* **54**, 379–387.

Ponte Castañeda, P. (1987c). Asymptotic analysis of a mode I crack propagating steadily in a deformation theory material. *J. Appl. Mech.* **54**, 79–86.

Ponte Castañeda, P. and Bose, K. (1990). Stable crack growth under mixed-mode conditions. Manuscript in preparation.

Rice, J. R. (1982). Elastic-plastic crack growth. In *Mechanics of Solids: The Rodney Hill 60th Anniversary Volume* (Edited by H. G. Hopkins and M. J. Sewell), pp. 539–562. Pergamon Press, Oxford.

Rice, J. R. (1988). Elastic fracture mechanics concepts for interfacial cracks. *J. Appl. Mech.* **55**, 98–103.

Rice, J. R., Drugan, W. J. and Sham, T. L. (1980). Elastic-plastic analysis of growing cracks. In *Fracture Mechanics: Twelfth Conf. ASTM-STP* 700, pp. 189–219. ASTM, Philadelphia.

Rice, J. R. and Sih, G. C. (1965). Plane problems of cracks in dissimilar media. *J. Appl. Mech.* **32**, 418–423.

Sham, T. L. (1983). A finite element study of the asymptotic near-tip fields for mode I plane strain cracks growing stably in elastic-ideally plastic solids. In *Elastic-Plastic Fracture: Second Symposium, Volume I—Inelastic Crack Analysis, ASTM STP* 803 (Edited by C. F. Shih and J. P. Gudas), pp. 52–79. ASTM, Philadelphia.

Shih, C. F. (1974). Small-scale yielding analysis of mixed mode plane-strain crack problems. In *Fracture Analysis, ASTM STP* 560, pp. 187–210. Philadelphia.

Shih, C. F. and Asaro, G. C. (1988). Elastic-plastic analysis of cracks on bimaterial interfaces. Part I: Small scale yielding. *J. Appl. Mech.* **55**, 299–316.

Shih, C. F. and Asaro, G. C. (1989). Elastic-plastic analysis of cracks on bimaterial interfaces. Part II: Structure of small scale yielding fields. *J. Appl. Mech.* **56**, 763–779.
Slepyan, L. I. (1973). Deformation at the edge of a growing crack. *Mekhanika Tverdogo Tela* **8**, 139–148.
Slepyan, L. I. (1974). Growing crack during plane deformation of an elastic-plastic body. *Mekhanika Tverdogo Tela* **9**, 57–67.
Williams, M. L. (1959). The stresses around a fault or crack in dissimilar media. *Bull. Seism. Soc. Am.* **49**, 199–204.
Willis, J. R. (1971). Fracture mechanics of interfacial cracks. *J. Mech. Phys. Solids* **19**, 353–368.
Zywicz, E. (1988). On elastic-plastic cracks between dissimilar media. Ph.D. Thesis, M.I.T., Cambridge.

APPENDIX A: THE GOVERNING SYSTEMS OF ODEs

Anti-plane strain

$$f_1 = (\sin\theta\, T_1)^{-1}[(s/\underline{\alpha})\cos\theta\, y_1 + \sin\theta\, T_2 y_2 + y_3]$$

$$f_2 = -(s+1)y_1$$

$$f_3 = -s^2\sin\theta\, y_1 - s^2\cos\theta\, y_2 - s(\underline{\alpha}^{-1}-1)T_3 y_2 + s(\underline{\alpha}^{-1}-1)\sin\theta\, \bar{y}_1\bar{y}_2 f_1$$

where

$$T_1 = [1+(\underline{\alpha}^{-1}-1)\bar{y}_1^2$$

$$T_2 = [1+(\underline{\alpha}^{-1}-1)(s+1)\bar{y}_1^2]$$

$$T_3 = [s\cos\theta + (s+1)\sin\theta\, \bar{y}_1\bar{y}_2]$$

and

$$\bar{y}_i = (y_i/y_e).$$

Plane strain

$$f_1 = (1-s)y_2 - 2s^2\cos\theta[(1+\nu)+(3/2)(\underline{\alpha}^{-1}-1)]y_3 - 2s\sin\theta\, T_1$$

$$f_2 = -y_1 - s^2\cos\theta[z_4 + (\underline{\alpha}^{-1}-1)x_4] - s\sin\theta\, T_2$$

$$f_3 = -(1+s)y_4 + y_5$$

$$f_4 = (1/\sin\theta)T_3\{\ldots\}$$

$$f_5 = -(s+2)y_3$$

$$f_6 = (1/\sin\theta)\, T_3\{\ldots\}$$

where

$$T_1 = s(1+\nu)y_4 - (3/2)(\underline{\alpha}^{-1}-1)\bar{y}_3 f_e$$

$$T_2 = sy_3 + \nu(f_4 - 2y_3 + f_6) - (\underline{\alpha}^{-1}-1)\bar{x}_5 f_e$$

$$T_3 = \{[1+(\underline{\alpha}^{-1}-1)\bar{x}_4^2][1+(\underline{\alpha}^{-1}-1)\bar{x}_6^2] - [\nu-(\underline{\alpha}^{-1}-1)\bar{x}_4\bar{x}_6]^2\}^{-1}$$

$$f_e = y_e'$$

$$x_4 = y_4 - (1/2)(y_5+y_6) \quad x_5 = y_5 - (1/2)(y_4+y_6) \quad x_6 = y_6 - (1/2)(y_4+y_5)$$

$$z_4 = y_4 - \nu(y_5+y_6) \quad z_5 = y_5 - \nu(y_4+y_6) \quad z_6 = y_6 - \nu(y_4+y_5).$$

APPENDIX B: THE PERFECTLY-PLASTIC SOLUTION FOR ANTI-PLANE STRAIN

Centered-fan plastic sector $(0 < \theta < \theta_1)$

$$\tau = \tau_0 \mathbf{e}_\theta$$

$$v_3 = -V(\tau_0/G)\sin\theta\ln r.$$

Elastic unloading sector $(\theta_1 < \theta < \theta_2)$

$$\tau = \tau_0[(C + B\ln|\sin\theta|)\mathbf{e}_1 + (A + B\theta)\mathbf{e}_2]$$

$$v_3 = V(\tau_0/G)B\ln r.$$

Constant stress sector $(\theta_2 < \theta < \pi)$

$$\tau = \tau_0\mathbf{e}_1$$

$$v_3 = V(\tau_0/G)B\ln r$$

where

$$A = \cos\theta_1 + \theta_1 \sin\theta_1$$

$$B = -\sin\theta_1$$

$$C = \sin\theta_1 [\ln|\sin\theta_1| - 1]$$

$$\theta_1 \approx 19.7112^\circ$$

$$\theta_2 \approx 179.6334^\circ.$$